Conotruncal Anomalies

14

Laura M. Mercer-Rosa and Meryl S. Cohen

Abbreviations

2D	Two-dimensional
AoV	Aortic valve
Asc	Ascending
AV	Atrioventricular
DORV	Double outlet right ventricle
DTG	Deep transgastric
IVC	Inferior vena cava
LAX	Long axis
LV	Left ventricle, left ventricular
LVOT	Left ventricular outflow tract
ME	Midesophageal
MPA	Main pulmonary artery
MAPCAs	Major aortopulmonary collateral arteries
PA	Pulmonary artery
RV	Right ventricle, right ventricular
RVOT	Right ventricular outflow tract
SAX	Short axis
SVC	Superior vena cava
TA	Truncus arteriosus
TEE	Transesophageal echocardiography
TG	Transgastric
TOF	Tetralogy of Fallot
TOF–PAtr	Tetralogy of Fallot with pulmonary atresia
TTE	Transthoracic echocardiography
UE	Upper esophageal
VSD	Ventricular septal defect

L. M. Mercer-Rosa (✉) · M. S. Cohen
Perelman School of Medicine, University of Pennsylvania, Philadelphia, PA, USA

Department of Pediatrics, Division of Cardiology, Children's Hospital of Philadelphia, Philadelphia, PA, USA
e-mail: mercerrosal@email.chop.edu

Key Learning Objectives

- Understand the applications of transesophageal echocardiography (TEE) in the assessment of conotruncal anomalies, such as tetralogy of Fallot, double outlet right ventricle, and truncus arteriosus
- Characterize these anomalies by TEE, including standard imaging planes used to visualize the anatomy
- Understand key components of the preoperative and postoperative TEE assessment of these malformations
- Recognize the role of TEE in defining problems associated with surgical repair of conotruncal anomalies

Introduction

Conotruncal malformations encompass a group of congenital heart defects with abnormal ventriculo-arterial connections. In this chapter, we address the most common conotruncal defects, namely, tetralogy of Fallot (TOF), truncus arteriosus (TA), and double outlet right ventricle (DORV), focusing on the applications of transesophageal echocardiography (TEE) in the assessment of these malformations. These cardiac defects comprise the vast majority of conotruncal abnormalities encountered by congenital heart disease specialists. Extremely rare conotruncal malformations, including anatomically corrected malposition of the great arteries and double outlet left ventricle, will not be addressed in this chapter. Transposition complexes such as *d*-transposition of the great arteries and congenitally corrected transposition are discussed separately in Chap. 15.

General Considerations

Echocardiography is an important diagnostic tool in patients with conotruncal abnormalities in a variety of settings. Conotruncal malformations are usually diagnosed prenatally or during the neonatal period by transthoracic echocardiog-

raphy (TTE). The transesophageal imaging approach becomes a powerful tool in the intraoperative setting. Preoperative TEE often provides additional anatomic information, a particularly important consideration when complex baffling procedures are being considered, and allows the echocardiographer to determine optimal views for imaging after the surgical intervention. This imaging approach is also of benefit in the assessment of the adequacy of the surgical repair for these lesions. This includes evaluation of residual intracardiac shunts, residual outflow tract obstruction, evaluation of atrioventricular and semilunar valve function, and assessment of ventricular performance. TEE is also essential in the evaluation of patients, particularly adolescents and adults, with poor transthoracic acoustic windows. Moreover, TEE represents an important imaging modality in the assessment of problems that may affect these patients such as in the evaluation of infective endocarditis and suspicion for intracardiac thrombus or aortic dissection, as discussed in Chaps. 19 and 20 [1, 2]. TEE is also helpful to facilitate catheter-directed interventions in these patients as addressed in Chaps. 21 and 22 [3, 4].

Specific Lesions

Tetralogy of Fallot

Anatomy
The classic four morphologic abnormalities that constitute the term "tetralogy" of Fallot (TOF) include an anterior malalignment-type ventricular septal defect (VSD), overriding of the aorta over the ventricular septum, subpulmonary stenosis, and right ventricular (RV) hypertrophy. Yet the fundamental anatomic defect in TOF is anterior malalignment of the infundibular (conal) septum. This malalignment results in a large, typically unrestrictive VSD with concurrent override of the aorta over the ventricular septum. Furthermore, the infundibulum (conal muscle under the pulmonary valve) is hypoplastic, with variable degrees of subpulmonary and pulmonary stenosis [5]. Right ventricular hypertrophy is a consequence of the large VSD—the RV being at systemic pressure—and the obstruction across the RV outflow tract (RVOT) [6].

TOF displays wide anatomic variation: from mild pulmonary stenosis to the most severe form, pulmonary atresia. In TOF with pulmonary atresia (TOF–PAtr), the anatomy of the PAs has a wide spectrum: from normal-sized, confluent PAs to diminutive or even non-existent pulmonary vessels with pulmonary blood flow supplied by way of major aortopulmonary collateral arteries (MAPCAs).

Known genetic abnormalities occur in 20% of patients with TOF [7]. The 22q11 deletion syndrome (including the DiGeorge and velo–cardio-facial syndromes) is seen in 15% of patients with TOF and is particularly common in those with associated arch sidedness abnormalities [8]. TOF is the third most common lesion in children with Down syndrome (trisomy 21) and is sometimes seen in association with endocardial cushion defect (atrioventricular canal or atrioventricular septal defect) in those patients [9]. Other conditions associated with TOF include VACTERL association and CHARGE syndrome. Patients with TOF and chromosomal anomalies tend to have worse outcome than those without genetic defects [7].

With the most common form of TOF (malalignment VSD and subvalvar/valvar pulmonic stenosis), surgery is usually performed within the first 6 months of life. Patients with mild to moderate pulmonary outflow tract obstruction may exhibit only a mild degree of cyanosis and arterial oxygen saturation can exceed 90% (so-called "pink TOF" variant). In this group, complete one-stage surgical repair can be electively performed at any time, usually around 6 months of age, sometimes even later. In other patients, surgical intervention is necessary at a younger age; indications for earlier repair include significant cyanosis and/or "tetralogy spells" characterized by acute, severe episodes of hypercyanosis [10–12]. For such patients, some institutions may utilize a staged approach. Surgical palliation to augment pulmonary blood flow may be performed with a modified Blalock-Taussig shunt. When the obstruction is primarily at the pulmonary valve level, some institutions may favor catheter-based approaches such as balloon pulmonary valvuloplasty, with or without stent placement across the RVOT as an alternative form of surgical palliation [13–15]. In either case, complete repair is undertaken several months later. Some centers yet prefer to perform a definitive, one-stage complete repair of TOF at a very young age, even during the neonatal period [16–18]. There is ongoing debate regarding the optimal approach to the symptomatic neonate with TOF [19, 20].

The surgical management of patients with TOF-PAtr is variable. Most will require some type of surgical intervention, and the timing of surgery can vary from the neonatal period to infancy or even to an older age. The surgical intervention is dependent on the anatomical subtype. Some patients are staged to complete repair: a modified Blalock-Taussig shunt or other type of aorto–pulmonary connection is performed in the neonatal period, followed by a complete repair, often with a RV to pulmonary artery (PA) conduit, within the first year of life. In some cases, initial palliation to establish a reliable source of pulmonary blood flow can be performed without surgery. This is achieved by interventional catheterization procedures such as stenting of the ductus arteriosus [21–23] and, when membranous pulmonary valve atresia is present, by radiofrequency perforation and dilation of the valve [24]. In more severe cases such as TOF-PAtr with MAPCAs, complex staged surgical palliation may be required including *unifocalization* of the aorto–pulmonary collateral vessels to a central location connected to a reliable source of pulmonary blood flow (Blalock-Taussig shunt or RV to PA conduit). It should also be noted that some

patients with TOF-PAtr and MAPCAs do not undergo any intervention throughout their lifetime. They continue to have lower than normal arterial oxygen saturations, but these remain compatible with survival because the aorto-pulmonary collaterals provide enough pulmonary blood flow to maintain an adequate systemic arterial oxygenation.

Transesophageal Echocardiographic Evaluation

Important aspects of the anatomy that should be considered in the TEE evaluation of patients with TOF and may impact the surgical intervention include:

- The presence of additional VSDs, typically in the muscular septum
- Absence or hypoplasia of the conal septum in addition to malalignment
- Restrictive VSD due to accessory tricuspid valve tissue
- Coronary anomalies, particularly a coronary artery crossing the RVOT, which occur in approximately 5% of TOF patients. These anomalies include variations such as origin of the left anterior descending coronary artery from the right coronary artery, dual left anterior descending coronary artery supply, and right coronary artery from the left anterior descending [25, 26].
- Persistent left superior vena cava (SVC), seen in 9–12% of patients [27, 28]. In these cases the left SVC usually drains into a dilated coronary sinus, but in rare instances it can return directly to the left atrium.
- Discontinuous PAs, whereby one PA originates from a ductus arteriosus or collateral vessel
- Common atrioventricular (AV) canal or septal defect, seen almost exclusively in Down syndrome
- Absent pulmonary valve leaflets—a subtype of TOF. The main features of this condition include an unguarded pulmonary valve annulus with massively dilated main (MPA) and proximal branch PAs. Free pulmonary insufficiency is invariably present, and airway compression is frequently found as well.
- Atrial septal defect or patent foramen ovale (the so-called pentalogy of Fallot)

Though the diagnosis of TOF is generally made using TTE, TEE can be helpful for confirmation of the diagnosis or in those patients with poor transthoracic acoustic windows. This includes the rare adult with unrepaired TOF [29]. The starting point is generally the midesophageal (ME) four-chamber (ME 4-Ch) view obtained with a transducer angle of ~0°–10°, which displays the four cardiac chambers, two AV valves, and may show the large malalignment VSD [30]. This view allows for assessment of the degree of RV hypertrophy and inspection of the atrial septum for any defects. As the probe is advanced and retroflexed to image posterior structures, the coronary sinus is viewed; it will be enlarged when connected to a persistent left SVC. As the probe is withdrawn, the malalignment VSD is
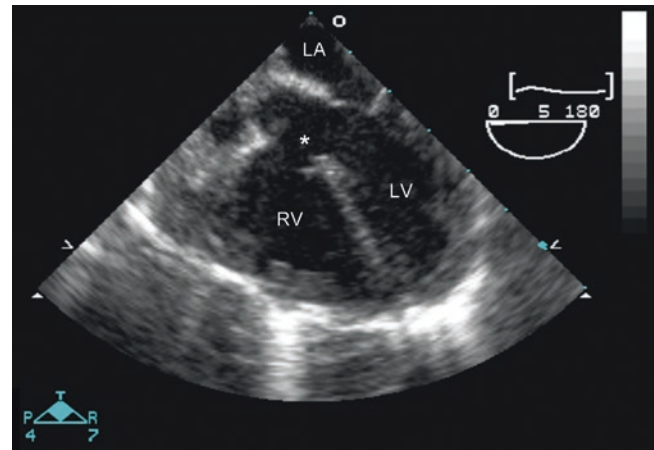
Fig. 14.1 ME 5-Ch view showing the large malalignment VSD (*asterisk*) and overriding aorta in TOF. *LA* left atrium, *LV* left ventricle, *RV* right ventricle

seen with the aorta overriding the ventricular septum in the ME five-chamber view (ME 5-Ch) at the same transducer angle of ~0°–10° (Fig. 14.1, Video 14.1). Further probe withdrawal and anteflexion demonstrates the hypoplastic pulmonary outflow tract. The atrial septum can be interrogated for a communication from an inferior to superior aspect in the ME 4-Ch view. The ME bicaval view (ME Bicaval), obtained at a transducer angle between ~90°–110°, allows for evaluation of the systemic venous connections (in a sagittal plane) and confirms the presence of an atrial communication, if present. The transducer angle can be maintained at 90° or rotated backward to 50°–70° to obtain the ME right ventricular inflow-outflow view (ME RV In-Out) in which the VSD is displayed as well as the anterior malalignment of the conal septum (Fig. 14.2, Video 14.2), stenotic pulmonary valve, and frequently hypoplastic MPA. As the probe is withdrawn into the upper esophagus, the proximal PA branches can be displayed by the upper esophageal (UE) PA view (UE PA; transducer angle of ~0°–20°). The TEE probe can then be advanced to the ME position and a transducer angle between ~120°–140° produces the ME long-axis (ME LAX) and ME aortic valve long-axis (ME AoV LAX) views. Both of these cross-sections can also be used to evaluate the VSD by two-dimensional (2D) imaging and all Doppler modalities, and the relationship of the overriding aorta to the VSD. Advancement into the stomach and probe anteflexion generates the deep transgastric (DTG) 5-Chamber (DTG 5-Ch; transducer angle of ~0°–20°) and the DTG right ventricular outflow tract (DTG RVOT; transducer angle of ~50°–90°) views. These views provide excellent visualization of the malalignment VSD, the overriding aorta, anteriorly malaligned infundibular septum, and narrowed RVOT (Fig. 14.3, Video 14.3). These cross-sections are similar to those obtained with the standard transthoracic subcostal coronal and sagittal views and sweeps.

Color Doppler evaluation prior to surgical intervention includes assessment of flow across the atrial septum (typical flow pattern is from the left atrium to the right atrium). The
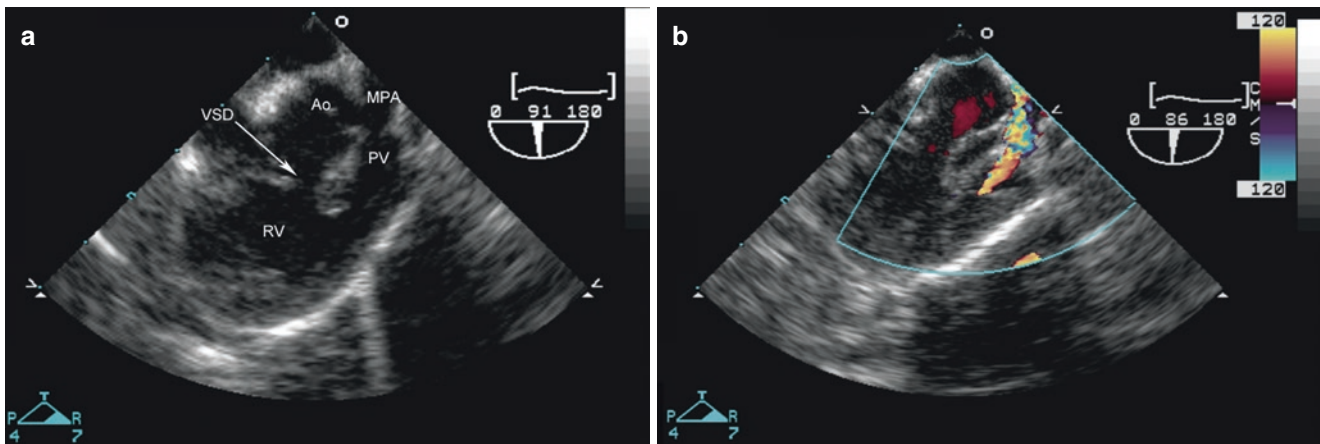
Fig. 14.2 *Panel* **a**, modified ME RV In-Out view (transducer angle of 91°) showing the ventricular septal defect (*VSD*) and narrowing of the RVOT due to the malaligned conal septum in TOF. *Panel* **b**, color flow Doppler shows aliasing beginning at the subpulmonary level and continuing across the hypoplastic pulmonary valve annulus. *Ao* aorta, *MPA* main pulmonary artery, *PV* pulmonary valve, *RV* right ventricle

ventricular septum should be interrogated in all views to assess for additional communications in the muscular septum as described in Chap. 10. Spectral Doppler determination of the peak velocity and derived gradient across the RVOT is best performed in the UE PA, ME RV In-Out (Fig. 14.2, Video 14.2), or DTG RVOT (Fig. 14.3, Video 14.3) views—whichever yields a more favorable angle for Doppler interrogation. To evaluate flow across the pulmonary valve and the branch PAs and to search for a possible patent ductus arteriosus, color Doppler can be performed using the UE PA and UE aortic arch short-axis (UE Ao Arch SAX; transducer angle of ~70°–90°) views. It should be remembered that a significant proportion of TOF patients with a right-sided aortic arch (present in about 25% of TOF) will have a left sided ductus arteriosus originating from the left subclavian or innominate artery, and entering the MPA or left PA [31].

Surgical Considerations

Intraoperative TEE should be performed in most patients undergoing TOF repair, unless there are contraindications, such as esophageal obstruction, unrepaired tracheoesophageal fistula or if the patient is too small for safe probe placement that would preclude an exam [30]. The usual operative repair of tetralogy of Fallot involves closure of the VSD (Figs. 14.4 and 14.5, Videos 14.4 and 14.5) and relief of the RVOT obstruction. The outflow tract surgery is dependent upon the severity of infundibular and pulmonary valvar hypoplasia. A transannular patch is used when the outflow tract obstruction is severe, with significant pulmonary valve hypoplasia. In milder forms of TOF, resection of infundibular muscle and patch enlargement of the hypoplastic infundibulum (an infundibular non transannular patch), is performed as required, preserving the pulmonary valve to avoid long-term issues related to pulmonary regurgitation (also known as 'valve-sparing repair') [32–34]. A transatrial approach may be employed, in which the VSD is closed through the right atrium, and the RV muscle is resected, thereby limiting the size or even avoiding a

right ventriculotomy [35, 36]. Conduit placement between the RV and PA is required in some cases, such as in most instances of TOF-PAtr or when a coronary artery crosses the RVOT (typically in the setting when a left anterior descending coronary artery originates from the right coronary artery). The coronary arteries can be evaluated preoperatively starting from the ME aortic valve short-axis view (ME AoV SAX) and navigating through other views as discussed in Chap. 17 [37]. With probe anteflexion and careful evaluation, it is possible to visualize a coronary artery crossing the RVOT (Figs. 14.6 and 14.7, Videos 14.6 and 14.7).

Postoperative TEE is helpful in the evaluation of:

- Residual RVOT obstruction
- Residual VSD(s) (Figs. 14.8, 14.9, 14.10, and 14.11, Videos 14.8, 14.9, and 14.10)
- Severity of pulmonary regurgitation
- Flow direction across the atrial septum (if a foramen ovale is intentionally left open)
- Severity of tricuspid valve regurgitation
- Ventricular performance

In the post repair assessment of all conotruncal malformations, corresponding TEE views should be used to assess for residual VSD as described in Chap. 10. The most common type of residual defect is a peri-patch leak between the sutures or at the margins of the defect (Fig. 14.8, Video 14.8). Defects smaller than 3 mm in size tend to have minimal hemodynamic impact, though some defects of that size can be a concern, particularly in very small infants [38]. Estimation of RV pressure either by Doppler interrogation of the tricuspid regurgitant jet velocity (if present) or of the residual VSD jet, particularly when the RVOT is unobstructed, is of utmost importance in assessment of hemodynamic significance of the residual VSD. By definition, a restrictive VSD is associated with an RV pressure that is subsystemic. At times an
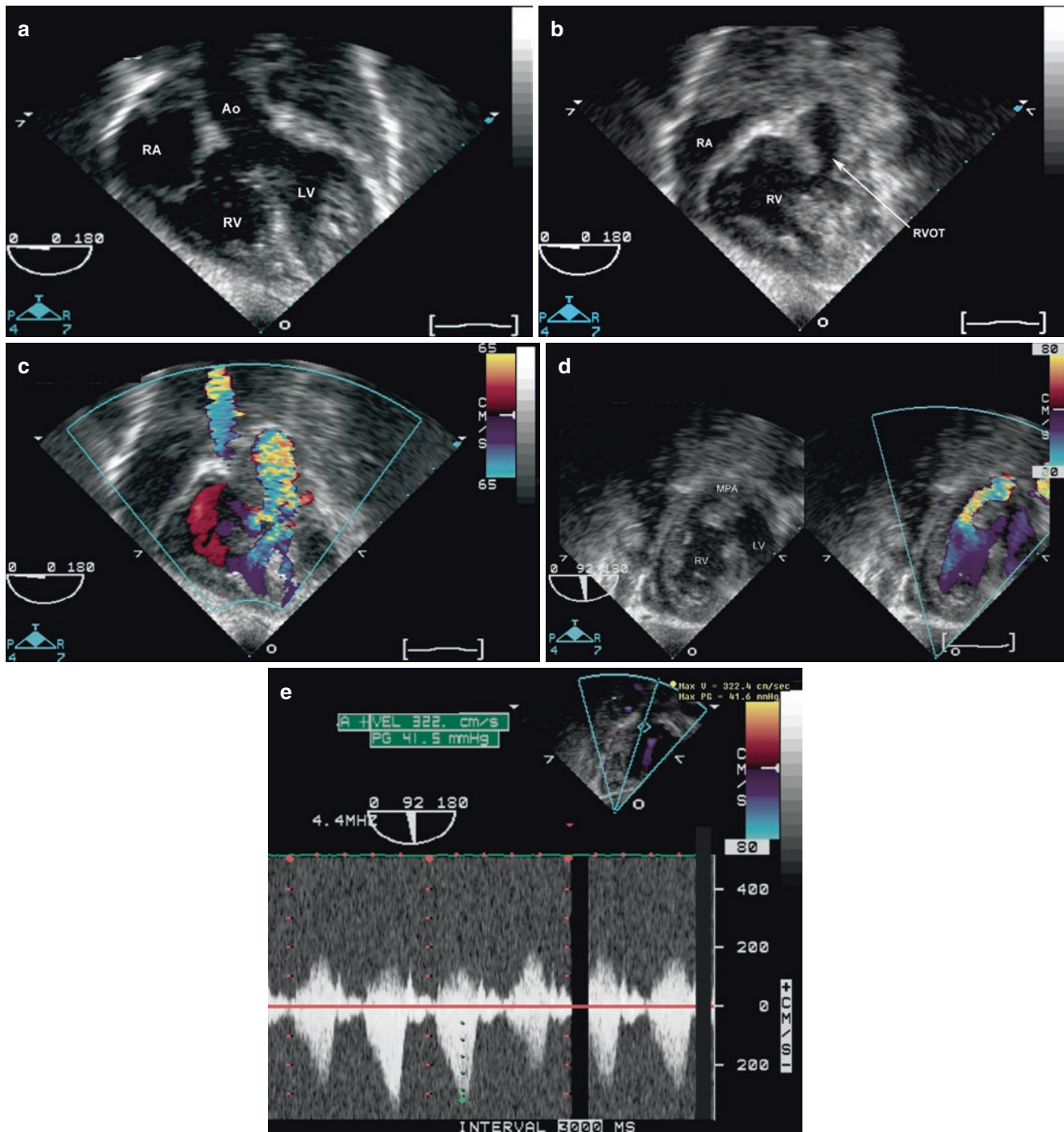
Fig. 14.3 Deep transgastric cross-sections in TOF simulating transthoracic subcostal coronal and sagittal views. *Panel* **a**, DTG 5-Ch view showing the malalignment VSD and overriding aorta. *Panel* **b**, with slight probe withdrawal, the anteriorly malaligned infundibular septum is seen by 2D imaging creating subpulmonary stenosis. *Panel* **c**, superimposed color flow in Fig. 14.3b showing aliasing across the RVOT. *Panel* **d**, DTG RVOT color compare image views showing the anteriorly malaligned infundibular septum with color flow aliasing, as well as the VSD with right-to-left shunting. *Panel* **e**, spectral Doppler tracing displaying the typical "dagger" shaped or late-peaking systolic flow signal associated with subpulmonary stenosis. *Ao* aorta, *LV* left ventricle, *MPA* pulmonary artery, *PV* pulmonary valve, *RA* right atrium, *RV* right ventricle, *RVOT* right ventricular outflow tract
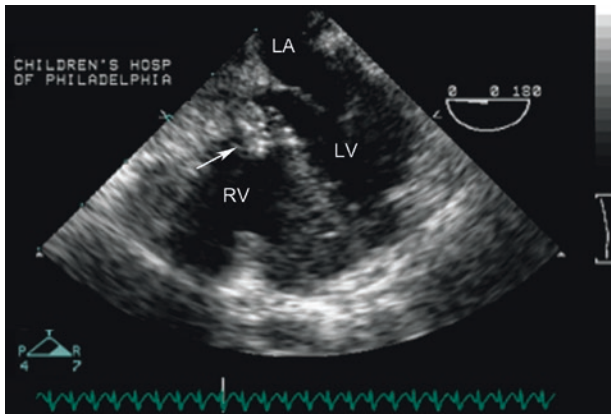
Fig. 14.4 ME 4-Ch view showing an echogenic VSD patch (*arrow*) in good position after repair of TOF. Note the hypertrophied RV. *LA* left atrium, *LV* left ventricle, *RV* right ventricle
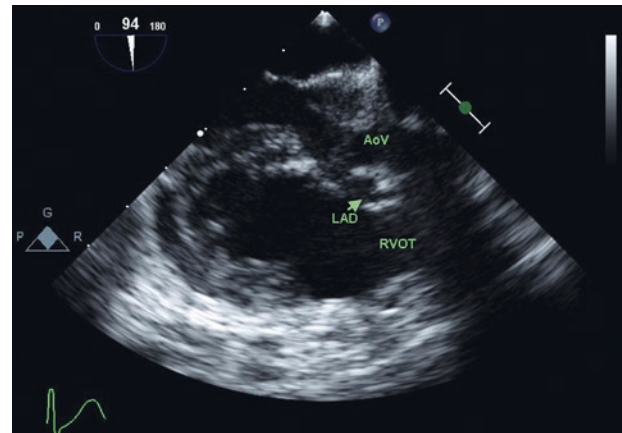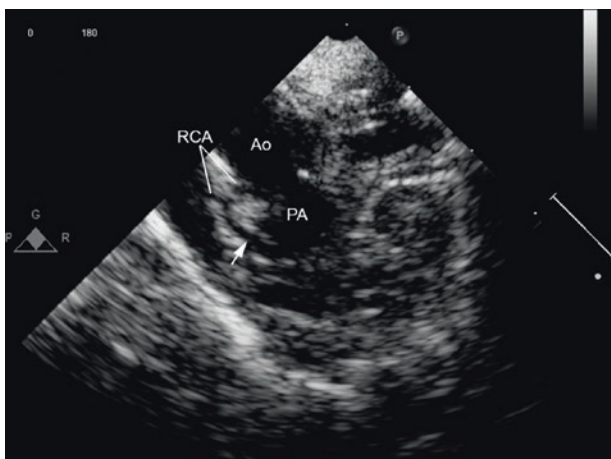

Fig. 14.7 ME LAX view showing the left anterior descending coronary artery (*LAD, arrow*) as it courses towards the right ventricular outflow tract (*RVOT*). *AoV* aortic valve

Fig. 14.5 ME RV In-Out view post TOF repair at a transducer angle of 79° showing an echogenic VSD patch and narrowing across the infundibular os by 2D imaging. *RVOT* right ventricular outflow tract
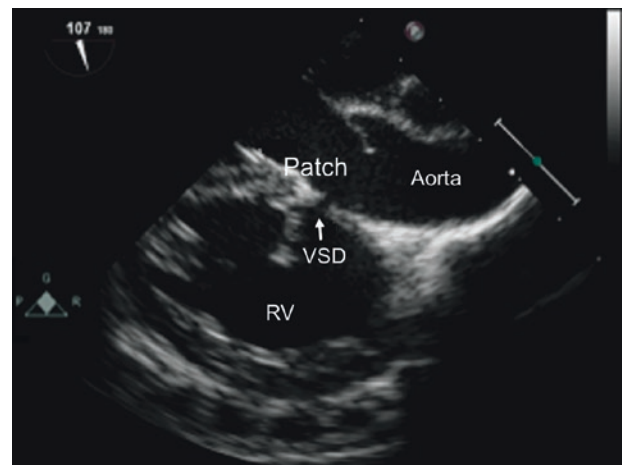
Fig. 14.8 Modified ME LAX view with a transducer angle of 107° in a patient post TOF repair showing a residual ventricular septal defect (*VSD*). The defect is located at the superior aspect of the patch just under the aortic valve. *RV* right ventricle

intraoperative direct assessment of the pulmonary to systemic blood flow ratio (Qp:Qs) is obtained, in which the surgeon directly obtains blood samples from the SVC and PA for co-oximetry, to determine hemodynamic significance of the residual ventricular communication. Epicardial echocardiography can be a useful complementary tool to TEE as it can help assess RV pressure and interrogate the branch PAs (the left PA in particular), which can be difficult by TEE [39–43].

One of the most challenging types of residual VSDs to assess comprehensively is the intramural defect. TEE has been shown to have modest sensitivity but high specificity in the identification of intramural VSDs and is considered to be able to detect most defects requiring reintervention [44]. This type of defect occurs in the setting of conotruncal malformations, when the VSD patch attaches to the RV trabeculations rather than the free wall related to the ventriculoinfundibular fold (parietal band) creating a com-
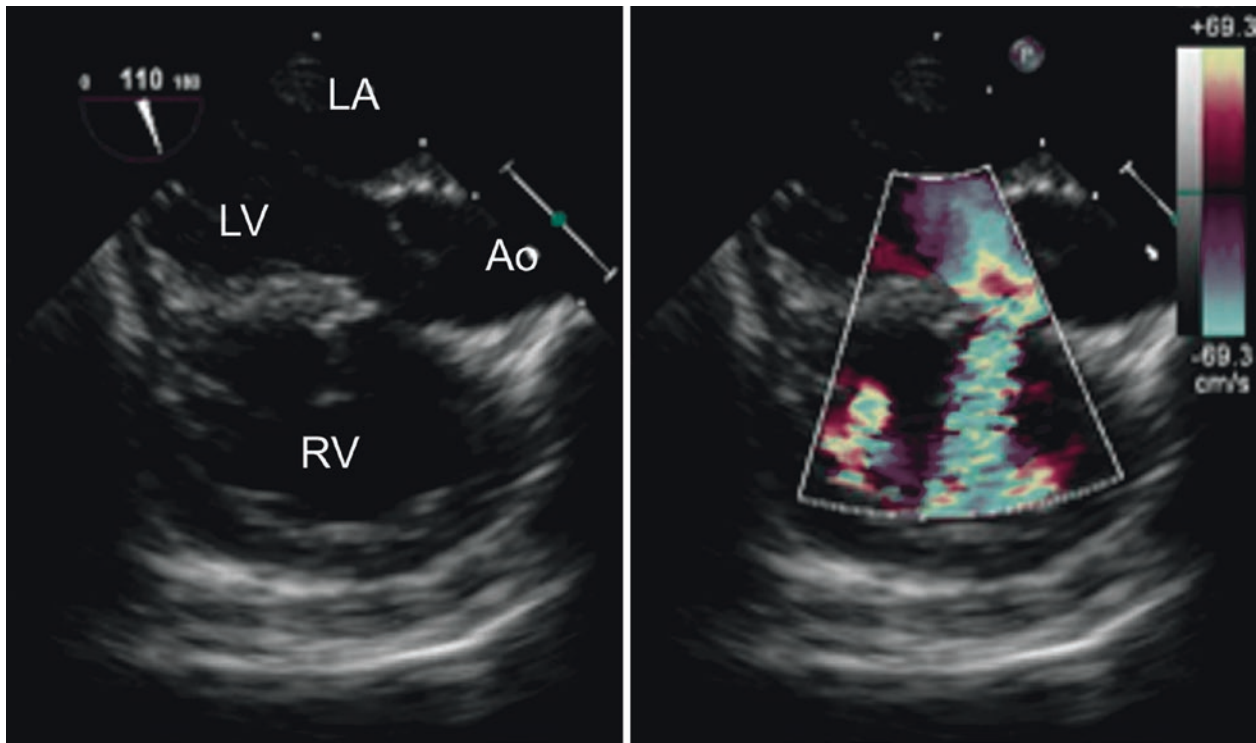

Fig. 14.6 Preoperative midesophageal view in a patient with TOF displaying the arterial roots. A prominent left anterior descending coronary artery (*arrow*) arises from the right coronary artery (*RCA*) and courses anterior to the RVOT, thereby precluding a transannular patch. *Ao* aorta, *PA* main pulmonary artery

Fig. 14.9 Modified ME LAX view color compare images (transducer angle of 110°) show a residual VSD after repair of TOF with left-to-right shunting. The defect, attributed to patch dehiscence, was located immediately below to the aorta. *Ao* aorta, *LA* left atrium, *LV* left ventricle, *RV* right ventricle
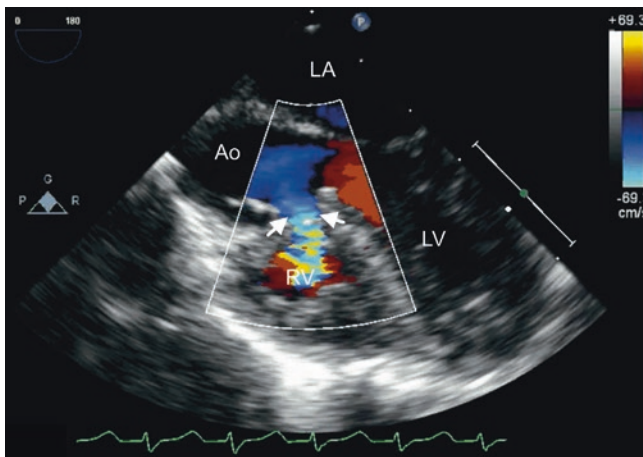
Fig. 14.10 ME 5-Ch view displaying a residual VSD after TOF repair (*arrows*). The defect appears at least moderate in size in this view. *Ao* aorta, *LA* left atrium, *LV* left ventricle, *RV* right ventricle
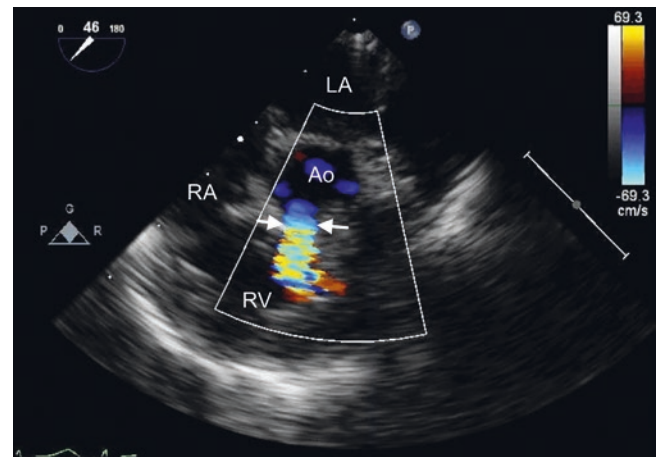

Fig. 14.11 ME RV In-Out view obtained in the patient displayed in Fig. 14.10 after TOF repair confirming the presence of the residual VSD (*arrows*). *Ao* aorta, *LV* left ventricle, *RA* right atrium, *RV* right ventricle

munication through the intertrabeculated spaces to the RV cavity (Fig. 14.12) [45, 47–49]. This region of the heart is difficult for the surgeon to visualize during the repair. Importantly, these defects can increase in size over time and become hemodynamically significant as the RV hypertrophy regresses with time [46]. Intramural residual VSDs should be examined for in all patients undergoing repair of conotruncal anomalies that include VSD closure. If found, another surgical approach might be necessary (e.g., through the AoV).

The ME 4-Ch, ME 5-Ch, and ME LAX views highlight this type of residual defect well, but it can also be seen in a modified ME RV In-Out view and from the DTG views (see case example #1). Refer to Chap. 10 for additional examples of intramural VSDs post repair of conotruncal defects.

Assessment of the RVOT for residual obstruction is best performed in the ME RV In-Out (Figs. 14.5, 14.13 and 14.14, Videos 14.5 and 14.11) and DTG RVOT views

a   b
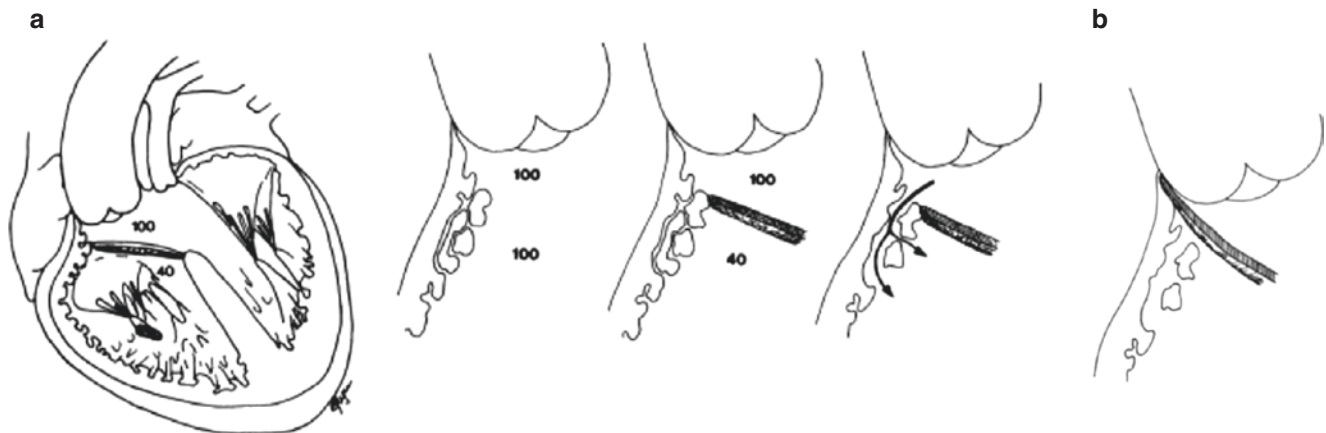
Fig. 14.12 *Panel* **a**, *left,* diagrammatic representation of intramural defects. The VSD patch is anchored to RV trabeculations rather than free wall; blood can pass between the trabeculae from the 'new' LVOT to the RV cavity. *Panel* **a**, *right,* magnified schematic representation of intramural defects. The channels might be small early after surgical repair of the conotruncal anomaly because of the RV hypertrophy; they enlarge subsequently to become hemodynamically significant with regression of hypertrophy after relief of the RV obstruction. From Preminger TJ et al. [45] with permission from Wolters Kluwer Health. *Panel* **b**, diagrammatic representation of optimal surgical positioning of the VSD patch required to achieve complete closure. From Patel JK et al. [46] with permission from Wolters Kluwer Health
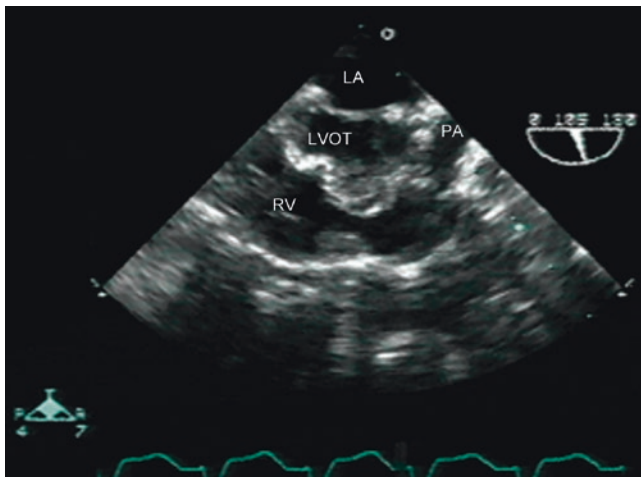
Fig. 14.13 Residual RVOT narrowing after TOF repair in a modified ME RV In-Out view. *LA* left atrium, *LVOT* left ventricular outflow tract, *PA* pulmonary artery, *RV* right ventricle
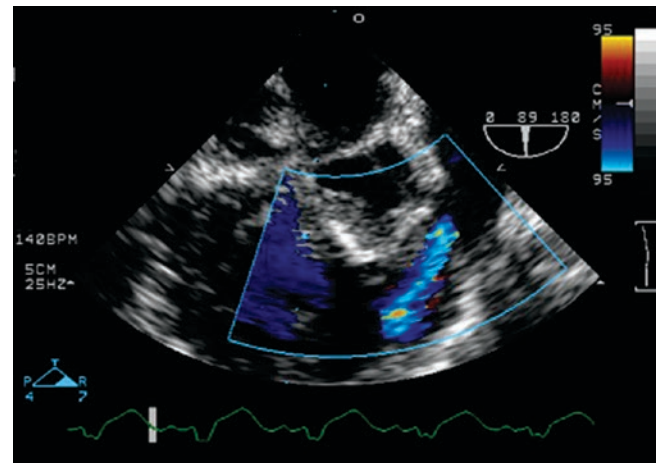
Fig. 14.14 Residual RVOT narrowing (arrow) after TOF surgery with color Doppler interrogation in a modified ME RV In-Out view. *Ao* aorta, *LA* left atrium, *MPA* main pulmonary artery, *RV* right ventricle

(Fig. 14.15, Videos 14.12 and 14.13), and their respective modifications. Doppler interrogation (color and spectral evaluation) should also be performed from the cross-sections allowed by these views. In cases where the outflow obstruction is located more inferiorly, the DTG RVOT view can be used for optimal Doppler evaluation. A peak Doppler velocity of more than 3 m/s (36 mm Hg) is considered potentially significant [50]. However, it should be noted that a hypercontractile state may exist immediately following TOF repair, potentially due to inotropic support, hypovolemia, and other factors that can accentuate a dynamic RVOT gradient. Indeed, a study by Kaushal et al. evaluating 166 TOF patients immediately following transatrial repair (median age 7 years) found that 35% of the cohort had "sig-

nificant" residual obstruction (gradient >40 mmHg, right:left ventricular pressure ratio > 85%). Most of these patients (88%) had a dynamic, rather than fixed, obstruction as defined by TEE; patients with fixed obstruction underwent immediate surgical revision, while those with dynamic obstruction did not. Operative mortality and morbidity were not related to higher residual gradients, and on follow-up (mean 18.5 months) outflow gradients had declined sharply (mean 16 mm Hg) irrespective of the severity of intraoperative gradients [51]. Thus, a "significant" gradient in the immediate postoperative should be viewed carefully; the nature of the obstruction (fixed vs. dynamic), and other intraoperative factors, should be considered when deciding to return to cardiopulmonary bypass to revise the repair.

Branch PA stenosis can be difficult to assess comprehensively using TEE [37], but in a number of instances can be performed using the ME and UE views and the techniques discussed in Chap. 4 (Fig. 14.16, Video 14.14). Epicardial echocardiography can also provide complementary information in this setting.

In addition to the evaluation of the surgical repair, TEE can be helpful in several aspects of the surgical intervention, including the process of cardiac de-airing prior to removal of the aortic cross-clamp. This is best accomplished using the ME 4-Ch and ME LAX views. The intraoperative evaluation of RV and left ventricular (LV) function can be performed from a number of ME and transgastric (TG) TEE views, including the ME 4-Ch, ME 5-Ch, ME two-chamber (ME 2-Ch; transducer angle of ~80°–100°), ME RV In-Out, and the TG basal (TG Basal SAX; transducer angle ~0°–20°) and mid papillary short-axis (TG Mid Pap SAX; transducer angle ~0°–20°) views. The LV outflow tract (LVOT) is well visualized in the ME 5-Ch (Fig. 14.17, Video 14.15), ME LAX

(Fig. 14.18, Video 14.16), and DTG 5-Ch views, although this rarely presents a problem after TOF repair [52].

Assessment of the severity of pulmonary regurgitation can also be performed using the same views that allow for evaluation of the RVOT, including the UE PA, UE Ao Arch SAX, ME RV In-Out, and DTG RVOT views. Some degree of pulmonary regurgitation can be expected after TOF repair, particularly following transannular patching. Several methods can be used to evaluate the severity of pulmonary regurgitation, including width of the color Doppler jet compared to outflow tract diameter (mild ≤1/3, moderate 1/3 to 2/3, severe ≥2/3) and presence of diastolic flow reversal in the branch PAs [53, 54]. However, changing hemodynamic and ventilatory conditions following TOF surgery can alter the amount of pulmonary regurgitation noted in the immediate postoperative period, compared to later in the patient's postoperative hospital course.

In some TOF patients, depending on institutional preference, a small atrial communication (usually in the form of a patent foramen ovale) is intentionally left patent as a "pop
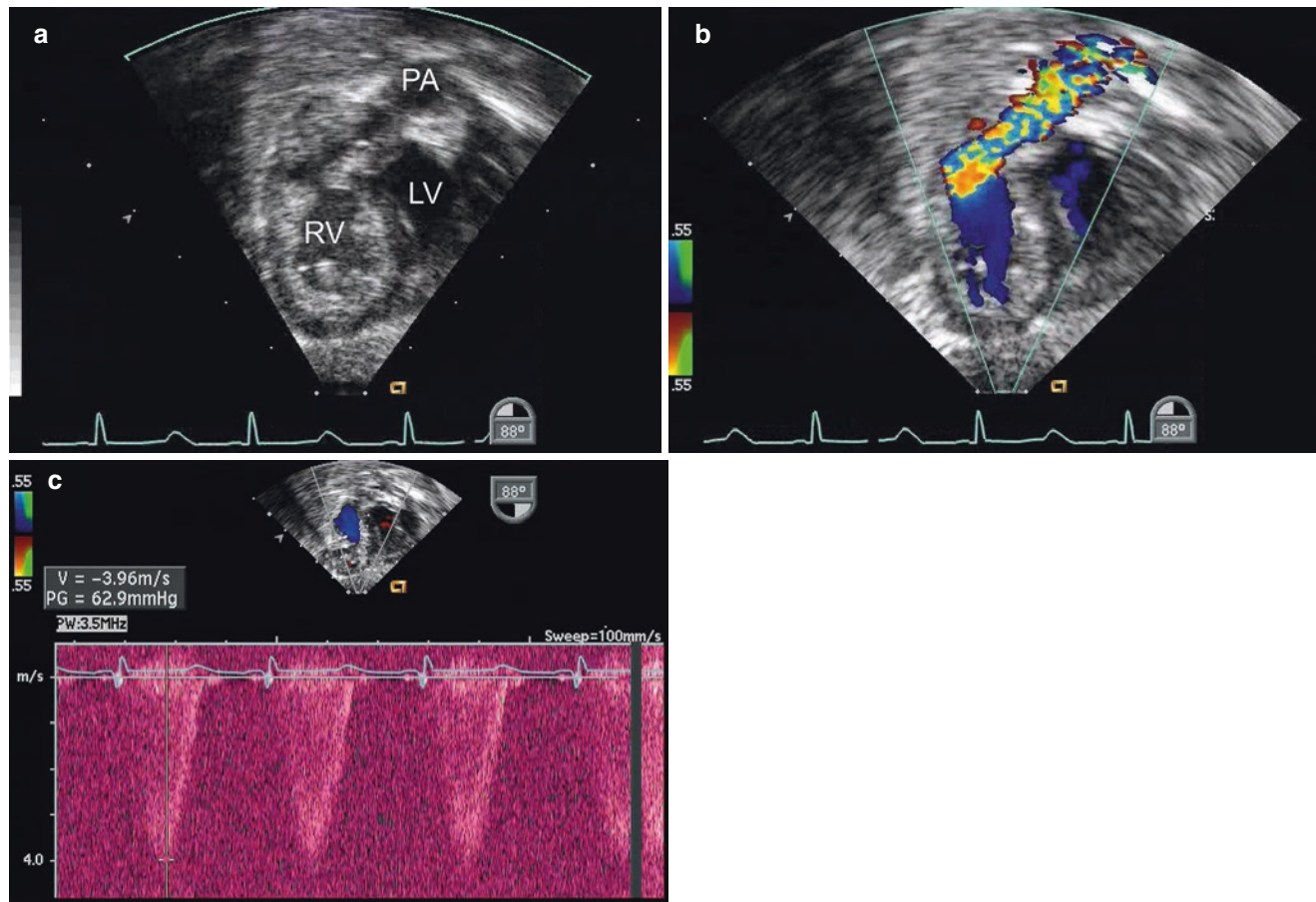

Fig. 14.15 *Panel a*, DTG RVOT view post TOF repair demonstrating significant residual muscular crowding across the RVOT by 2D imaging. *Panel b*, corresponding color Doppler image showing aliased flow across the RVOT consistent with residual obstruction. *Panel c*, spectral Doppler interrogation (note the optimal cursor alignment) depicting a peak residual pulmonary outflow tract gradient of ~63 mmHg, minimally changed from the preoperative study. Based on these findings, cardiopulmonary bypass was reinstituted. *LV* left ventricle, *PA* pulmonary artery, *RV* right ventricle
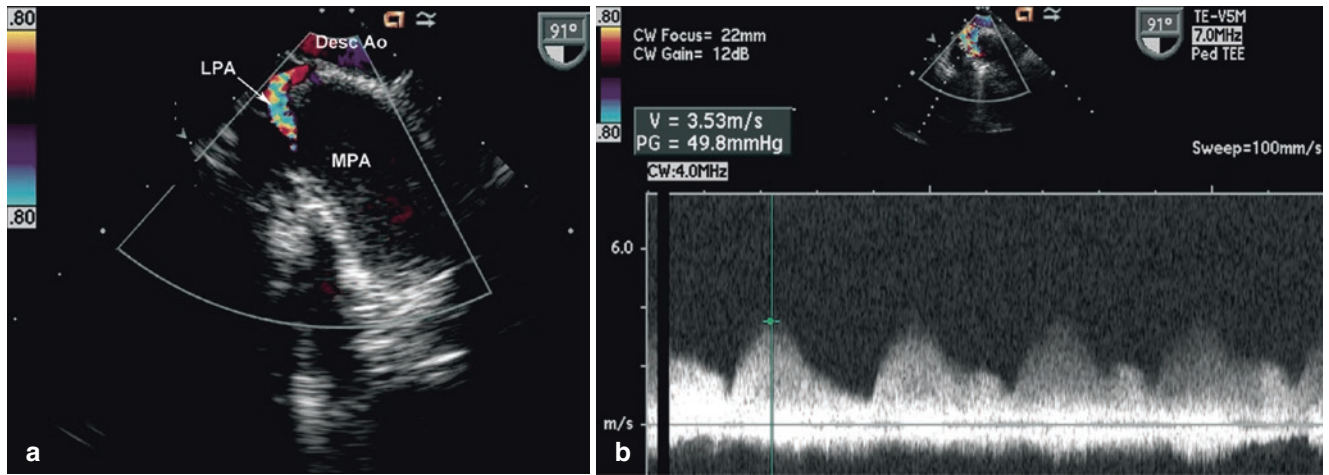
Fig. 14.16 *Panel* **a**, UE Ao Arch SAX view with counterclockwise rotation, demonstrating significant left pulmonary artery (*LPA*) hypoplasia by color Doppler imaging post complete repair of TOF that included repair of disc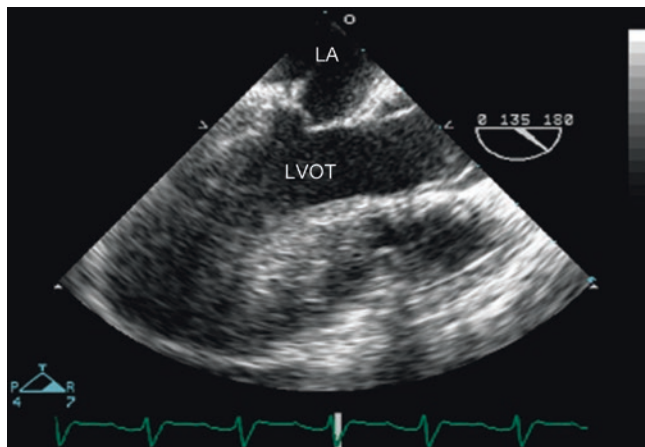ontinuous pulmonary arteries. *Panel* **b**, continuous-wave spectral Doppler tracing shows a significant gradient across the stenotic vessel with continuous flow throughout the cardiac cycle. *Desc Ao* descending aorta, *MPA* main pulmonary artery
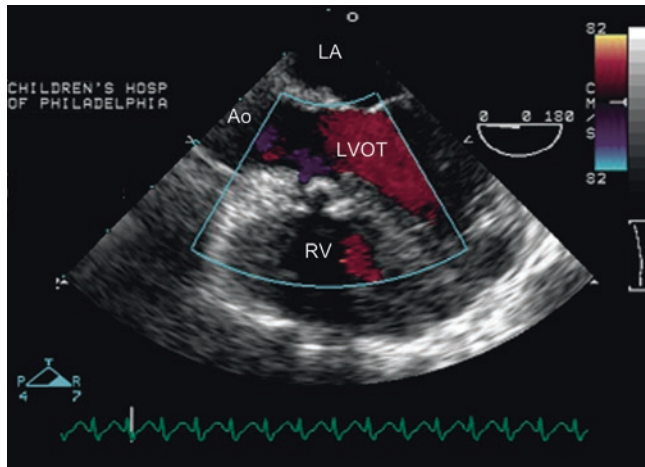
Fig. 14.17 ME 5-Ch view after repair of TOF showing laminar flow across the left ventricular outflow tract (*LVOT*). *Ao* aorta, *LA* left atrium, *RV* right ventricle
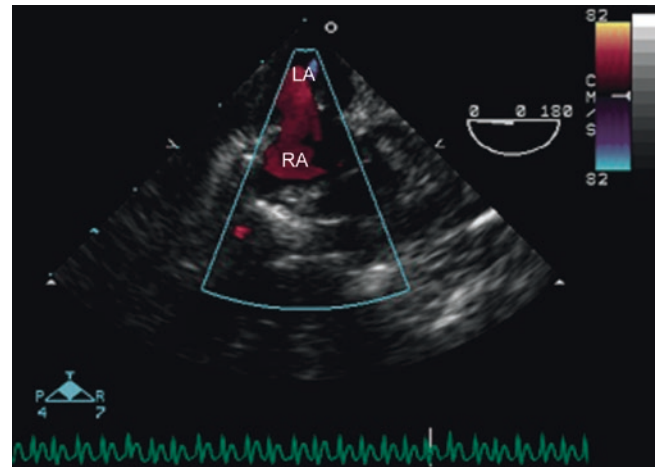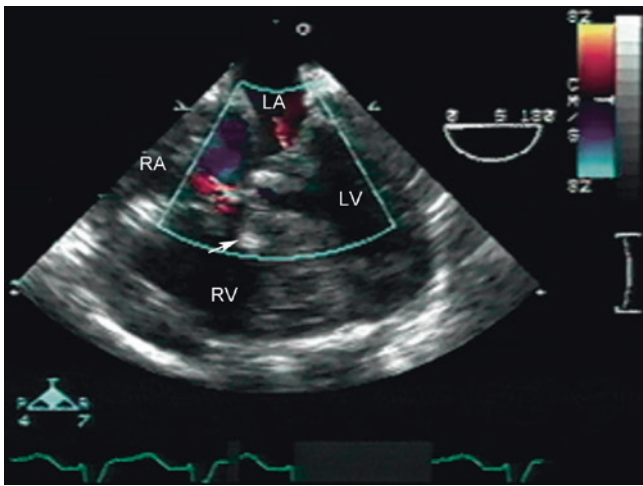

Fig. 14.19 ME 4-Ch view with color flow Doppler across the atrial septum demonstrates right-to-left shunting (red flow) through a large patent foramen ovale after repair of TOF. *LA* left atrium, *RA* right atrium

off" to assist in supporting cardiac output during the immediate postoperative period. The blood flow pattern across the foramen ovale after surgery for TOF may be from the right atrium into the left atrium as a result of diminished RV diastolic compliance, related to the right ventriculotomy and RV hypertrophy (Fig. 14.19). The atrial septum can be evaluated by sweeping from the inferior vena cava (IVC) to the superior vena cava. This sweep is performed by starting from the TG IVC/hepatic veins view (TG IVC/Hep veins), obtained at a transducer angle of ~80°–100°, then slowly withdrawing the probe to the ME Bicaval view. The ME 4-Ch view (with slight rightward probe rotation) also allows for visualization of the atria and atrial septum after rotating the transducer angle backward to between ~0°–30°.


Fig. 14.18 ME LAX view depicting an unobstructed left ventricular outflow tract (*LVOT*) after repair of tetralogy of Fallot. *LA* left atrium

Fig. 14.20 ME 4-Ch view post repair of TOF and atrioventricular canal defect. A VSD patch is seen (*arrow*). Small jets of atrioventricular valve regurgitation are noted. *LA* left atrium, *LV* left ventricle, *RA* right atrium, *RV* right ventricle
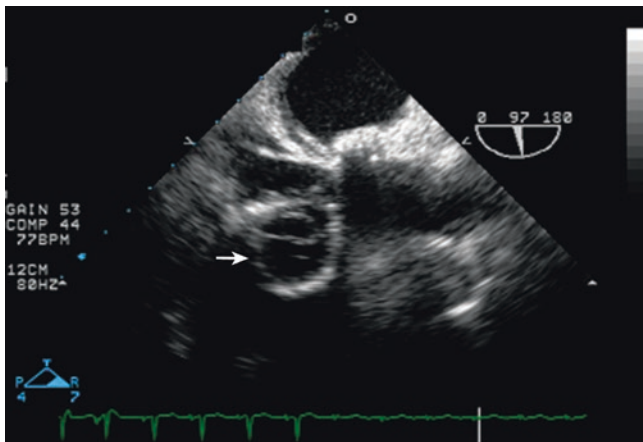
Fig. 14.21 Severe tricuspid regurgitation prompted valve replacement in this adult long after TOF repair. The bioprosthetic valve appears in cross-section as indicated by the *arrow* in this modified ME RV In-Out view (transducer angle of 97°)

In the case of the patient with TOF and an AV canal (AV septal) defect, both atrial and ventricular septal patches should be evaluated for residual shunts. As with all AV septal defect repairs (Chap. 8), both AV valves (particularly the left AV valve) should be evaluated for possible regurgitation and stenosis (Fig. 14.20, Video 14.17). In addition, the RVOT and all pertinent aspects of the repair should be evaluated in the same manner as any other patient with more common forms of TOF.

In adult patients with TOF and those with poor acoustic windows, TEE can be used as indicated during follow up to assess the repair. The long-term impact of severe pulmonary regurgitation can be gauged by evaluation of RV size and performance as described in Chap. 5, although in most cases magnetic resonance imaging is the favored diagnostic imaging modality. When there appears to be significant negative impact of the regurgitation (manifested by marked RV dilation and/or deteriorating RV or LV systolic function), pulmonary valve replacement may be indicated. This can be performed either surgically or in some cases the pulmonary valve can be implanted via a transcatheter-based approach [55–57]. Tricuspid valve repair or replacement may be indicated in cases of severe tricuspid regurgitation (Fig. 14.21, Videos 14.18 and 14.19). Right ventricular systolic pressure estimates can be performed using the peak velocity of the tricuspid regurgitation jet, if present. Aortic root dilation is a common finding in adults with TOF and can be associated with the development of aortic regurgitation over time. The aortic valve, root, and ascending aorta can be assessed in short- and long-axis views by multiplane imaging (refer to Chap. 4) These cross-sections, along with those that display the LVOT are also helpful in the evaluation of aortic valve regurgitation.

Patients with TOF can also develop important dysrhythmias such as ventricular tachycardia. The use of an onscreen electrocardiogram is very helpful in these situations. In some cases, TEE can help distinguish between the various dysrhythmias. This can be accomplished by monitoring atrial and ventricular contraction for signs of synchronous/dyssynchronous contraction, and also whether there is a 1:1 correspondence between the atrial and ventricular chambers. In the case of atrial flutter/fibrillation or complete heart block, the atrial rate can be seen as much more rapid than the ventricular rate, and there will not be coordinated contraction between the atria and ventricles. In the case of ventricular tachycardia, the ventricles will be seen to contract at a very rapid rate, much faster than the atria, and with a lack of coordination between the atrial and ventricular chambers.

Double Outlet Right Ventricle

Anatomy
Double outlet right ventricle (DORV) is not a specific congenital malformation, but rather, an abnormal ventriculo-arterial alignment whereby both great arteries arise from the morphologic RV [58, 59]. By most criteria, both great vessels must sit more than 50% over the RV [60]. Typically, there is *bilateral conus (infundibula)*, with myocardium separating both great vessels from the AV valves. However, other conal anatomy can occur in DORV [61]. A VSD is present in almost all cases and usually acts as the "outlet" from the LV. However, there are rare reports of DORV with an intact ventricular septum [62, 63]. In DORV, the ventricular loop may be "D" (normal) or "L" (inverted) and this will affect the relationship of the great arteries to the ventricles and to each other.

The anatomic and physiologic spectrum of DORV is wide. Associated anomalies are common and include ven-

tricular hypoplasia, superior/inferior ventricles, mitral valve anomalies (including mitral atresia, straddling or parachute mitral valve), common AV canal (in heterotaxy syndrome), and outflow obstruction [61, 64, 65].

The pathophysiology in DORV can be similar to TOF, transposition of the great arteries, or a large VSD. This physiology is determined by the location of the great vessels in relationship to the VSD and the degree of outflow obstruction. Of critical importance is the type and location of the VSD: it often determines the type of surgical repair as well as, in some instances, the suitability for two-ventricle versus a single ventricle surgical strategy [66, 67]. By far, the most common type of VSD in DORV is the malalignment type, however any type of VSD (such as AV canal, perimembranous, doubly committed, mid muscular, or apical muscular) can occur [68]. The VSD is classified as one of four types, based upon its relationship to the great vessels: subaortic, subpulmonary, non-committed (remote), and doubly-committed. In those patients with DORV with malalignment type VSD, the most common location of the VSD is subaortic. If there is no pulmonary stenosis, the physiology is similar to that of a large unrestrictive VSD because the blood flow streams from the LV into the pulmonary artery. If there is pulmonary stenosis, the physiology is similar to TOF. However, the distinction between DORV and TOF is of utmost importance because those patients with TOF-like DORV have a complete subaortic conus that can result in subaortic obstruction after surgery [69]. Subaortic stenosis is extremely rare in TOF.

The most common form of DORV with subpulmonary VSD is classically termed a "Taussig-Bing" anomaly [70, 71]. In this defect, the great vessels are spatially oriented side-by-side, bilateral conus is present, and the aorta is to the right of the PA. The blood from the LV streams into the PA so that the physiology is similar to *d*-transposition of the great arteries (refer to Chap. 15). The rightward, anteriorly malaligned conal septum often causes subaortic muscular narrowing, thus aortic arch obstruction is a frequent association. Some cases of DORV with subpulmonary VSD are not classic Taussig-Bing anomalies but rather fall within the spectrum of that anatomic description. The distinction is critically important when determining surgical strategy [72].

More uncommon locations of the VSD in DORV include non-committed or doubly-committed subtypes. In DORV with non-committed VSD, the VSD is usually a muscular, perimembranous, or a canal (inlet)-type VSD. Since it is far from both outflow tracts, baffling procedures may pose a significant challenge. Often, AV valve tissue is obstructing the potential pathway from the LV to the aorta. Moreover, straddling of the tricuspid valve can occur in association with a canal-type VSD. When a muscular VSD is present, there is a tendency for the defect to become progressively smaller over time because it is surrounded by muscle; therefore, in general a muscular VSD is not considered a reliable pathway for outflow to a great artery. In the rare doubly-committed type of VSD, both great vessels are situated directly over the ventricular communication, which is of the malalignment-type, and there is generally a deficient conal septum that allows the VSD to be anatomically related to both outflow tracts. Nonetheless, some degree of aortic or pulmonary stenosis can still be present. Repair of these defects can be performed by intraventricular tunnel repair, although LVOT obstruction with this type of repair is a risk [73] [74].

Other variations of DORV exist, most commonly including those with mitral atresia or hypoplasia associated with LV hypoplasia. When there is significant ventricular hypoplasia, the single ventricle palliation strategy is most likely indicated. DORV is often seen in patients with superior/inferior ventricles with criss-cross AV valves. In this rare anomaly, the RV is situated superior to the LV and it is typically hypoplastic. The VSD can be inlet or malalignment-type.

Genetic syndromes can be seen with DORV. In particular, 22q11 deletion has been reported in these patients, although it may be less common when compared to other conotruncal anomalies. Transforming growth factor (TGF)-beta 2 knockout mice have been observed to develop DORV in the majority of cases [75]. Heterotaxy syndrome often has DORV as one of its cardiac components.

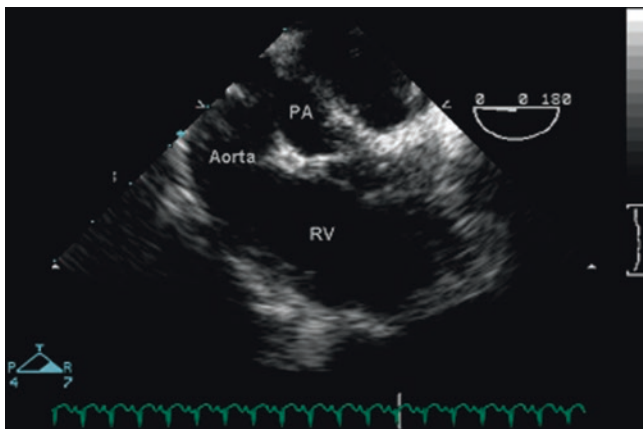## Transesophageal Echocardiographic Evaluation

Important aspects of the anatomy that should be considered in the TEE evaluation of DORV and may impact the surgical intervention include:

- Location, size, and number of VSD(s)
- Relationship of great vessels to the VSD
- Presence of additional VSDs
- Restriction of the VSD due to accessory AV valve tissue
- Anatomy and size of the AV valves, including straddling or overriding
- Presence and severity of outflow tract obstruction (and to which great vessel)
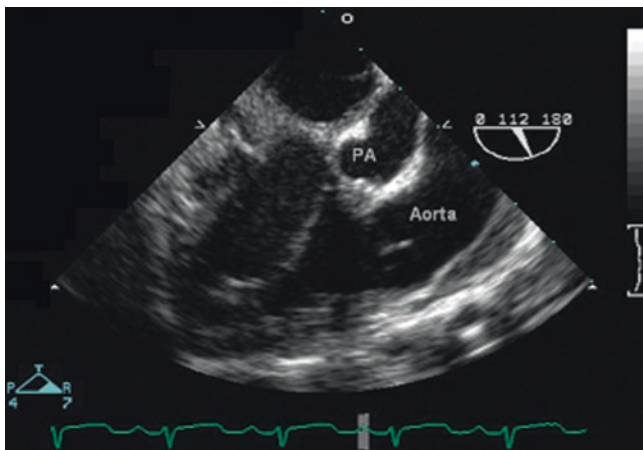- Coronary artery anatomy, particularly if an arterial switch operation is being considered

One of the most important aspects of the preoperative evaluation in the patient with DORV is assessment of location and size of the VSD(s) and its relationship to the great vessels. Alignment of the great vessels is dependent on their position; therefore, no single TEE view will be adequate for all patients with DORV. This evaluation requires multiple views and in particular sweeps that display the ventriculo-arterial relationships. The multiplane probe allows for the best view of the outflow tracts to be determined as the study is being performed. The standard ME 4-Ch view may not show evidence of pathology other than RV hypertrophy. However, probe withdrawal and anteflexion to obtain a ME 5-Ch view will demonstrate both great vessels arising mostly or completely arising from the anatomic RV in DORV (Fig. 14.22,

Video 14.20). ME LAX views complement this assessment (Figs. 14.23 and 14.24). The DTG views (DTG RVOT and DTG 5-Ch) are key in visualizing the great arteries as they arise from the RV (Fig. 14.25), their relationship to the VSD, and assessing outflow tract patency (Fig. 14.26, Video 14.21). Additional VSDs can be identified in the ME 4-Ch, ME 5-Ch, ME LAX, and ME RV In-Out views, with variations of the standard transducer angles and axial probe rotation to perform a complete sweep of the ventricular septum. The TG short-axis views (TG Basal SAX and TG Mid Pap SAX) are also useful in the evaluation of additional VSDs. TEE can also assess whether a VSD is restrictive and the mechanism of restriction (i.e., AV valve tissue, conal muscle) [76, 77].

A number of important anatomic features are also relevant in the determination the optimal surgical strategy in DORV. These include the pathway that allows for outflow of the ventricles into the great arteries, presence of tricuspid valve attachments to the conal septum, and the distance between the pulmonary and tricuspid valves, depending on the anatomic substrate [78]. The conal septum can represent a significant contributor to outflow obstruction in some cases (Fig. 14.27, Video 14.22). The evaluation of outflow tract obstruction requires 2D assessment and the application of all Doppler modalities. Three-dimensional (3D) echocardiography can also contribute to this evaluation in older children when the use of the 3D TEE probe is feasible.
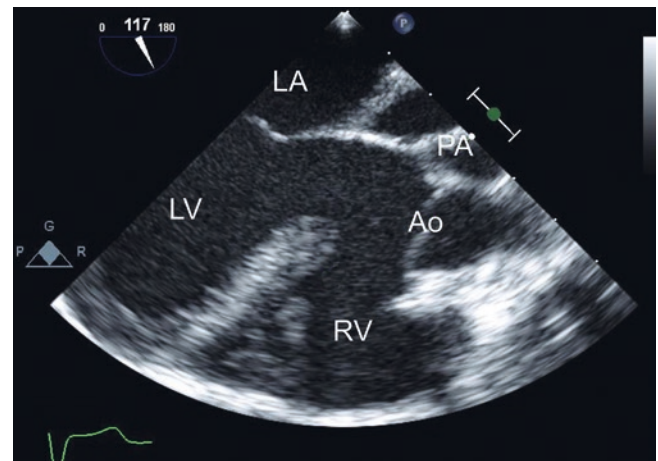

Fig. 14.22 ME view with the probe withdrawn towards the base of the heart in a patient with DORV, posterior malalignment of the conal septum, and a subpulmonary VSD. In this image, the aorta and pulmonary artery (*PA*) both arise from the right ventricle (*RV*). The PA is smaller than the aorta due to the conal septal malalignment

Fig. 14.24 ME LAX view in a patient with DORV and doubly-committed VSD. Note absence of conal septum between the great arteries. This view complements others in the preoperative assessment of the relationship between the VSD and outflow tracts. *Ao* aorta, *LA* left atrium, *LV* left ventricle, *PA* pulmonary artery, *RV* right ventricle
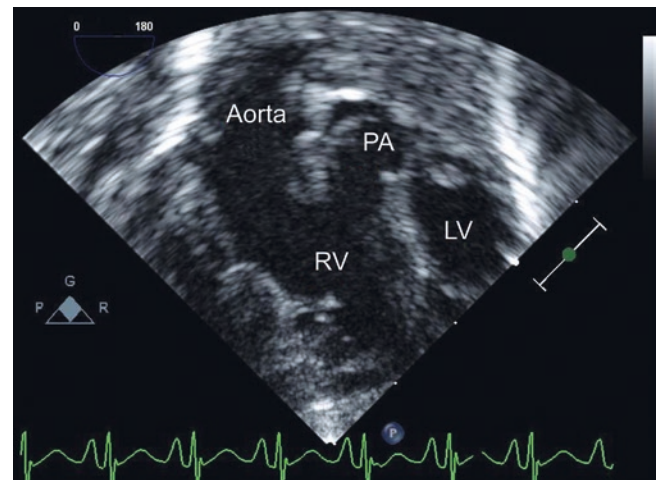

Fig. 14.23 ME LAX view in same patient displayed in Fig. 14.22 with DORV, showing an anterior aorta to the smaller pulmonary artery (*PA*). Both great vessels arise from the anterior RV. The conal septum is seen between the aorta and PA


Fig. 14.25 DTG 5-Ch view displaying origin of both great arteries from the right ventricle (*RV*) in DORV. A prominent conal septum is seen. This view allows for visualization of the ventriculo-arterial connections and facilitates the assessment of the relationship of the VSD to the great arteries. *LV* left ventricle, *PA* pulmonary artery
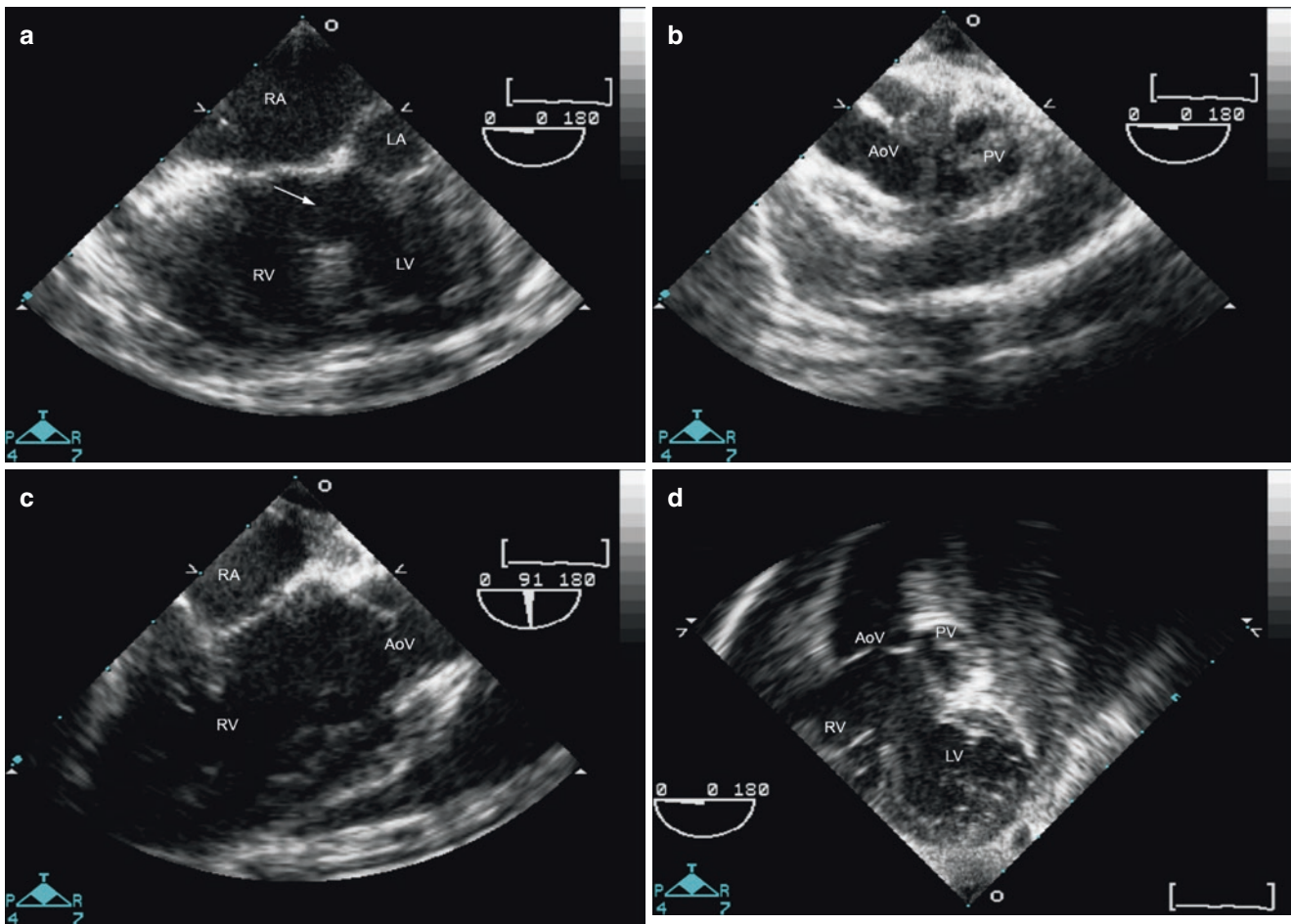
Fig. 14.26 DORV with pulmonary stenosis. *Panel* **a**, ME 4-Ch view showing a large VSD (*arrow*). *Panel* **b**, with probe withdrawal and anteflexion, the aortic valve (*AoV*) and pulmonary valve (*PV*) are visualized. *Panel* **c**, with forward rotation of the transducer angle to 91° a view is displayed showing the right atrium (*RA*) and right ventricle (*RV*) as well as the AoV. *Panel* **d**, DTG 5-Ch view showing an unobstructed pathway between the left ventricle (*LV*) and AoV
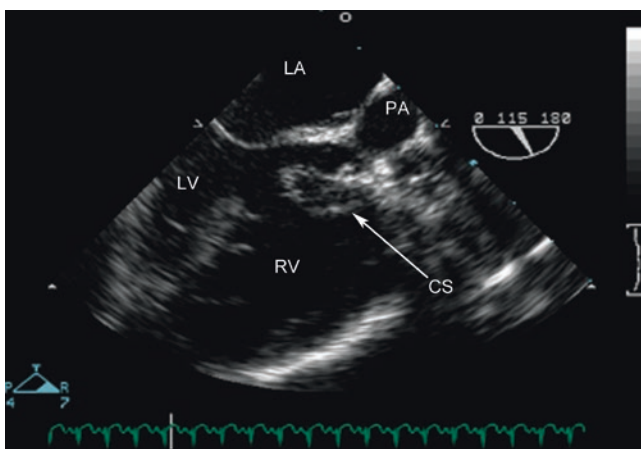
Fig. 14.27 ME LAX view in the same patient displayed in Fig. 14.22 and 14.23 with DORV, highlighting the location of the VSD in relationship to the pulmonary artery (*PA*) and the posterior deviation of the hypertrophied conal septum (*CS, arrow*) resulting in severe subpulmonary stenosis. *LA* left atrium, *LV* left ventricle, *RV* right ventricle
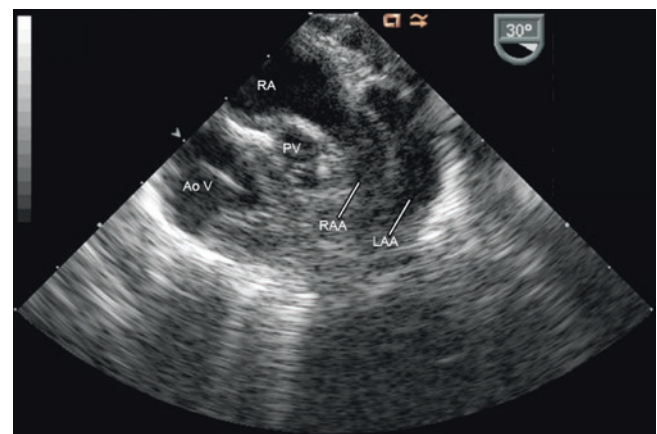
Fig. 14.28 Midesophageal view at 30° displaying left juxtaposition of the atrial appendages in a patient with DORV and pulmonary stenosis. Note how the right atrial appendage (*RAA*) lies just anterior to the left atrial appendage (*LAA*). *AoV* aortic valve, *RA* right atrium, *PV* pulmonary valve

TEE is an excellent tool to assess for AV valve abnormalities that might preclude a biventricular repair. For example, a straddling AV valve over the VSD usually obstructs the pathway from the LV to a great artery. Other associated anomalies can be demonstrated using TEE, including an AV canal defect (as is common in heterotaxy syndrome), as well as juxtaposition of the atrial appendages, which can be seen from a modified ME 4-Ch view as well as in a ME AoV SAX view (Fig. 14.28, Video 14.23; also refer to Chap. 7). Systemic venous connections can be evaluated using the TG IVC/Hep veins and DTG atrial septal (DTG Atr Sept; transducer angle ~80°–90°) views, as well as the ME Bicaval view (Chap. 4). Pulmonary venous connections can be evaluated using the views and examination sequence described in Chaps. 4 and 6.

Color Doppler is essential in the assessment of preoperative AV and semilunar valve stenosis/regurgitation as well as to evaluate flow across the VSD in order to exclude restriction. This interrogation is also useful to assess the inflow across each ventricle, particularly when hypoplastic, straddling, or overriding AV valves are suspected. Pulsed- and continuous-wave Doppler assessment of outflow tract obstruction is influenced by the angle of interrogation. The DTG RVOT and DTG 5-Ch views can be very helpful for optimal spectral Doppler angle alignment. LV systolic pressure estimate (as measured by mitral regurgitation jet) is important if a restrictive VSD is suspected. The LV can be at suprasystemic pressure in this setting. This method of assessment, performed with the ME 4-Ch and ME 2-Ch views, is particularly important when the VSD jet is not at an optimal angle for spectral Doppler interrogation.

Surgical Considerations

In some cases, initial palliation requires PA banding or a systemic-to-pulmonary shunt. When both ventricles and both AV valves are well developed, the goal of surgical repair is to utilize the VSD to baffle or direct flow from the LV to one of the great arteries. If baffled to the aorta, a "physiologic repair" is achieved. If baffled to the PA, an arterial switch operation is required. In cases where the VSD is remote from the great arteries, ventricular septation might not be possible or may require complex intracardiac baffling. In addition, the presence of a straddling tricuspid valve over a canal-type VSD or straddling mitral valve over a malalignment VSD can also preclude septation into two ventricles. In these cases, staged surgical palliation culminating in the Fontan operation may be required [79].

For patients undergoing a biventricular repair, selection of the appropriate surgical strategy depends upon an assessment of the great artery relationship to the ventricles and the VSD, whether outflow tract obstruction is present and if so, which outflow tract is obstructed and to what degree. Based upon these assessments, a determination can be made as to the most suitable operation to allow for a complete biventricular repair. Surgical procedures for DORV include:

- Patch closure of the VSD (baffle allowing for closure of the VSD and at the same time redirection of blood flood from the LV into the aorta)
- Rastelli type procedure or equivalent such as REV operation: intraventricular repair with baffle closure of VSD to aorta, reconstruction of obstructed RVOT (RV to PA conduit or outflow patch)
- Arterial switch operation with closure of the VSD to the neo-aorta
- Nikaidoh operation with translocation of the aorta into the pulmonary position over the LV, VSD closure, and placement of an RV to PA conduit [80–83]. This operation is designed to bring the aorta and aortic valve closer to the LV, thus reducing the risk of postoperative LVOT obstruction. (Fig. 14.29, Video 14.24).
- Other operations include the Yasui procedure in the setting of systemic outflow tract obstruction with two adequate ventricles. This allows for a biventricular repair leaving the LV as the systemic pump, by tunneling the VSD towards the pulmonary valve, performing a Damus-Kay-Stansel anastomosis, and placing an RV to PA conduit [84, 85].

The postoperative TEE evaluation is dependent upon the surgical intervention. In patients with a subaortic VSD, the two most important issues are assessment for residual ventricular level shunting and determination of possible LVOT obstruction across the baffle from the LV into the aorta. The subaortic conus as well as the position of the VSD patch may result in significant subaortic obstruction. The best view to
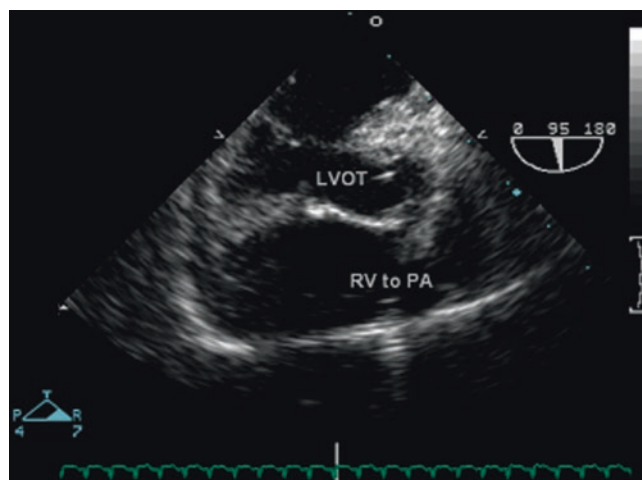
Fig. 14.29 ME LAX view in the patient shown in Figs. 14.22, 14.23, and 14.27 with DORV, posterior malalignment of the conal septum with subpulmonary VSD after the Nikaidoh procedure. Translocation of the aorta has placed the aortic valve closer to the left ventricle, improving left ventricular outflow tract (*LVOT*) alignment and reducing the possibility of subaortic obstruction after VSD patch closure. This image demonstrates the "physiologic" repair achieved by closing the VSD to the aorta in its new position and placing a right ventricular (*RV*) to pulmonary artery (*PA*) conduit

assess the LVOT is variable, depending on the relationship of the aorta to the LV. Though the ME LAX, ME AoV LAX, and ME 5-Ch views are best for a normal LVOT, this may not be the case in DORV, thus trying different TEE views, probe rotations, and transducer angles will often be required to obtain the best image. Doppler interrogation of the outflow tracts can also be challenging. A variety of different TEE views will often be necessary to obtain the optimal Doppler angle of interrogation; these usually include a combination of ME, TG, and DTG views. Severity of the obstruction may also have to be determined by other methods such as smallest diameter. In some cases, direct pressure measurements in the LV and the aorta might be required.

Assessment for residual ventricular communications is very important in patients undergoing repair of DORV. Intramural-type defects can occur in this lesion as can be the case following TOF repair as previously described (Fig. 14.30, Videos 14.25 and 14.26). In patients with Taussig-Bing anomaly that undergo the arterial switch operation, the intraoperative TEE examination includes evaluation of residual intracardiac shunting, patency of outflow tracts, AV and semilunar valve competency, global and regional ventricular function, as well as adequacy of the repair of associated defects, as described in Chap. 15 on transposition complexes.

When complete repair is not possible, or a decision is made to defer the repair until a later time in infancy (such as in cases of DORV with little or no pulmonary stenosis and development of congestive heart failure) banding of the PA may be undertaken [86]. Intraoperative TEE in this setting can be performed to assess the position and gradient across the PA band. This is best achieved using the UE PA, ME RV In-Out, and DTG RVOT views, as these allow for optimal
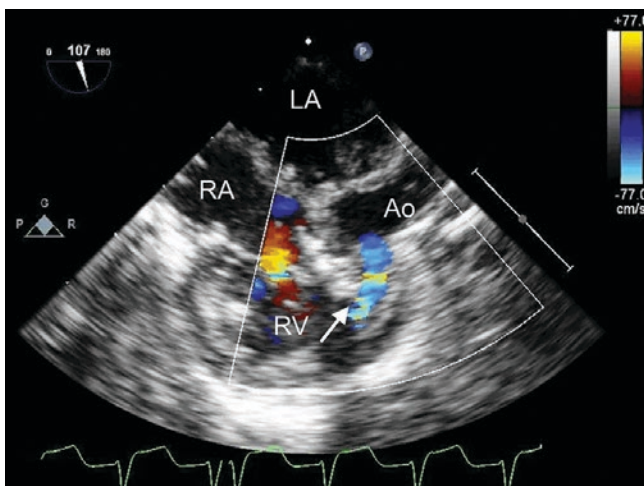
Fig. 14.30 Image obtained as the TEE probe is rotated to 107° to display the RV after the first revision of a residual intramural VSD in a patient with DORV. Note that residual left-to-right ventricular level shunting is still present (arrow). *Ao* aorta, *LA* left atrium, *RA* right atrium, *RV* right ventricle

spectral Doppler assessment. Intraoperative epicardial echocardiography can also inform the position and gradient across the PA band [30, 39, 43].

TEE plays an important role in the evaluation of adult patients with complications associated with DORV such as: outflow tract obstruction (left and right), RV to PA conduit failure (stenosis or regurgitation), aortic valve regurgitation, endocarditis, intracardiac thrombus or thromboembolic event, coronary artery stenosis, and ventricular failure.
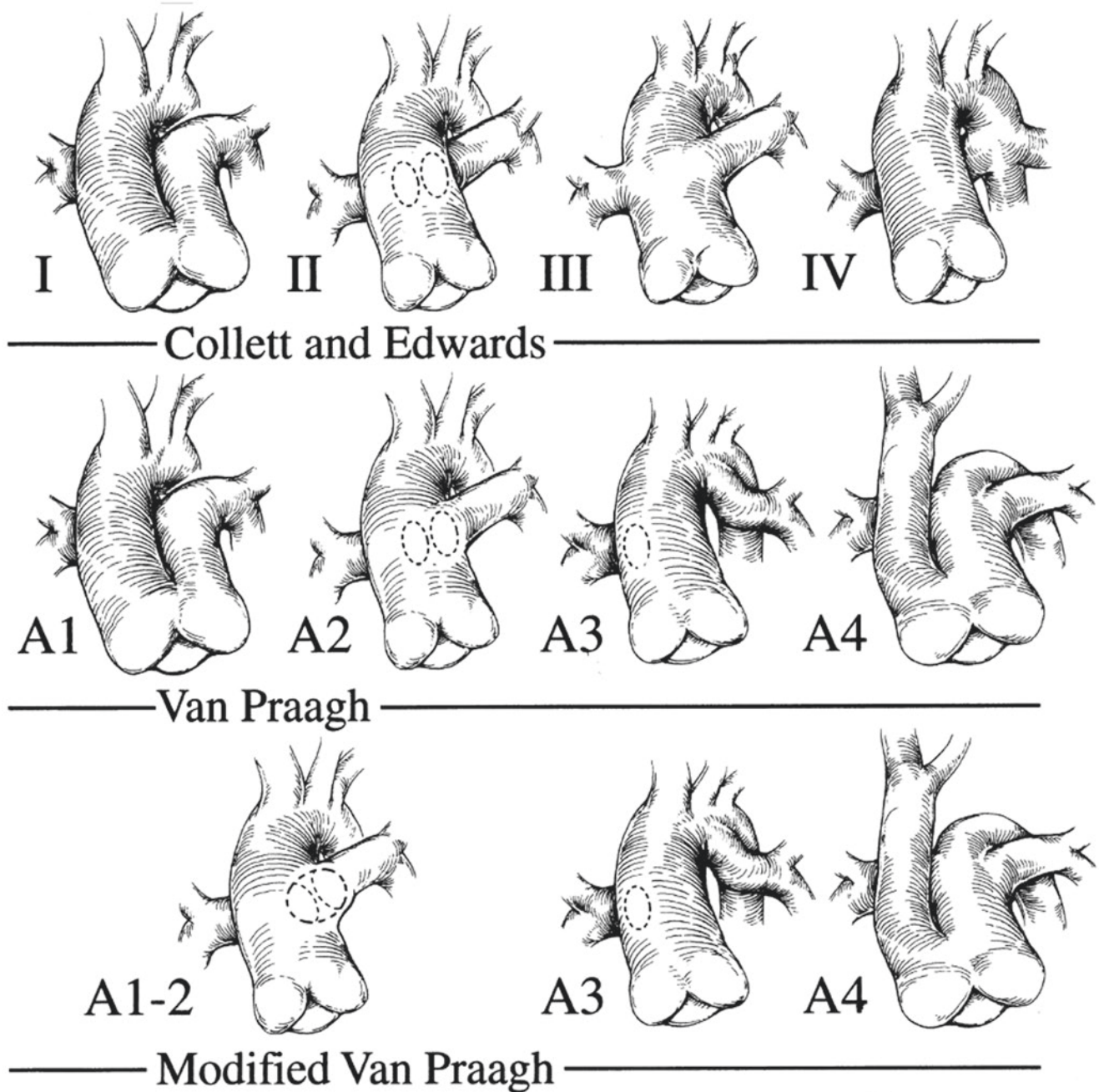
Truncus Arteriosus

Anatomy

Truncus arteriosus communis, also known more simply as truncus arteriosus (TA) or common arterial trunk, is characterized by a solitary great vessel that arises from the heart, giving rise to the aorta, at least one PA, and at least one coronary artery. Almost always, there is a large VSD in which the septal band (septomarginal trabeculation) forms the "floor" of the VSD, and the truncal root overrides the crest of the ventricular septum so that the solitary truncal valve forms the "roof" of the VSD [87]. The morphology of the VSD in TA is similar to that of TOF [88], but in TA the infundibular or conal septum is absent. However, in contrast to TOF, the posterior limb of the septal band is usually well developed. Truncus arteriosus must be distinguished from TOF-PAtr. In the latter a remnant of the valve and MPA can often be seen, however in some cases there is no well-developed MPA and the distinction between TA and TOF-PAtr can be challenging.

In TA, the solitary semilunar valve, the truncal valve, is often morphologically abnormal. Though a tricuspid truncal valve is the most common anatomic subtype (69%), other variations can occur including (in order of frequency), quadricuspid (22%), bicuspid (9%), and rarely valves with five leaflets (0.3%) [89]. Because of these frequent abnormalities in valvar anatomy, associated truncal valve stenosis and/or regurgitation are common, and if clinically significant, they may need to be addressed surgically. Approximately 25% of patients with TA have a right aortic arch [90]. Other associated cardiac anomalies include aberrant origin of a subclavian artery from the descending aorta, persistent left SVC draining to the coronary sinus, coronary artery anomalies, and an atrial communication in the form of a patent foramen ovale or secundum atrial septal defect. There have been rare reports of TA in the setting of a single ventricle [91]. In the absence of aortic arch obstruction, a ductus is rarely seen in this lesion.

Two classification schemes have been proposed for this malformation: one described by Collett and Edwards [92] and the other by Van Praagh [88, 93]. Both are based principally upon the manner in which the PAs arise from the truncal root. The classifications share similarities although there are also some important differences (Fig. 14.31).

Fig. 14.31 The two common classification systems for truncus arteriosus: Collett and Edwards (*first row*) and Van Praagh (*second row*) are shown. A modified Van Praagh classification system is noted on the *third row*. From Jacobs ML [94] with permission from Elsevier

The Collett and Edwards classification is as follows:

- Type I: There is partial absence of the aorto-pulmonary septum, and a short MPA segment (of variable length) that arises from the common trunk and gives rise to the branch PAs This is the most common type, comprising 48–68% of all TA.
- Type II: There is total absence of the aorto-pulmonary septum and the PAs arise directly from the posterior aspect of the common trunk. This type comprises 29–48% of all TA.

- Type III: The branch PAs arise separately from the common trunk and are remote from each other. The type comprises 6–10% of all TA.
- Type IV: The pulmonary circulation derives from the collateral arteries arising from the descending aorta. This type is now considered a form of TOF-PAtr and aortopulmonary collaterals, and is not generally used as a classification for TA.

The Van Praagh classification is listed below:

- Type A1: There is partial absence of the aorto-pulmonary septum: there is an MPA segment (of variable length) that arises from the common trunk and gives rise to the branch PAs.
- Type A2: There is total absence of the aorto-pulmonary septum and the PAs arise directly from the posterior aspect of the common trunk.
- Type A3: One of the PAs arises directly from the common trunk and one arises directly from a collateral supply (usually the ductus arteriosus). This is also known as truncus with absent PA.
- Type A4: Truncus arteriosus in association with interruption of the aortic arch. The common trunk gives rise to the ascending aorta and MPA, from which the ductus arteriosus and the branch PAs arise. The transverse arch is absent, thus there is an interrupted aortic arch. The ductus arteriosus provides blood supply to the descending aorta, thus this type of TA represents a ductal-dependent lesion. The interruption is usually type B (between the left carotid and the left subclavian arteries). This type occurs in 13% of cases.

Of note, the original Van Praagh classification scheme provided a subclassification of each type: A (with a VSD) and B (no VSD). Thus, a Type 1 TA could be divided into Type A1 and Type B1, depending upon the presence/absence of a VSD. However, given the fact that a VSD is almost always present, the Type B subclassifications are rarely seen. The reader will also note that the first two types of TA for both classification schemes are essentially identical; these are by far the common types of TA encountered. Another important point is that many TA patients are classified as "Type I" when, in reality, the two PA orifices are located so close together that no MPA segment is present. This type is often referred to as "truncus arteriosus Type I–II" or "Type 1½" [94].

Genetic syndromes are quite common in patients with TA. In fact, 40% have 22q11 deletion syndrome; this association is particularly high in those with a right aortic arch [90]. Other chromosomal defects such as isochromosome 8q have been implicated as well [95].

**Transesophageal Echocardiographic Evaluation**

Important aspects of the anatomy and function that should be considered by TEE in TA include:

- Assessment of the VSD and evaluation for potential additional VSDs
- Evaluation of truncal valve anatomy and function
- Determination of the origin of both PAs from the common trunk as well as their anatomy (including presence/absence of stenosis)
- Evaluation of AV valve function
- Evaluation of ventricular systolic function
- Comparison of ascending aorta to MPA size. In Type 1 TA (Type A1 of Van Praagh), the ascending aorta is generally much larger than the MPA segment. However in TA patients with an interrupted aortic arch (Type A4 of Van Praagh), the ascending aortic diameter will usually be smaller than that of the MPA [88, 93, 96].
- Assessment of other possible cardiac abnormalities, including atrial septal defects, systemic/pulmonary venous anomalies, and possible coronary artery anomalies.

TEE can be very helpful in the preoperative evaluation of the patient with TA. A comprehensive TEE study serves to evaluate all of the elements listed above. The ME 4-Ch view provides for evaluation of AV valve function and global assessment of ventricular performance. Withdrawal of the probe with anteflexion will demonstrate the truncal valve in the ME 5-Ch view. Forward transducer angle rotation to ~30°–45° will often display the truncal valve anatomy *en face* and assist in the assessment of cusp number and motion (Fig. 14.32, Video 14.27). An important aspect of the examination is the evaluation of valve function to determine presence and severity of stenosis, regurgitation, or both. The use of multiple views and all available Doppler modalities (spectral and color Doppler) is essential to accomplish this goal.

The VSD can be visualized in orthogonal planes in the ME 5-Ch (using probe anteflexion or withdrawal once the ME 4-Ch view is obtained), ME AoV SAX (Fig. 14.33, Video 14.28), and ME LAX views. In Type I or II TA, these same views along with the ME ascending aortic short-axis (ME Asc Ao SAX; transducer angle ~0°–30°) and ME ascending aortic long-axis (ME Asc Ao LAX; transducer angle ~120°–140°) views, will often demonstrate the PAs
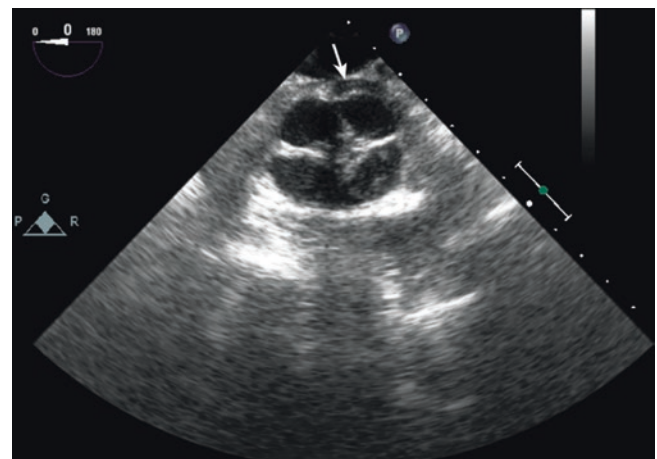
Fig. 14.32 Truncal valve shown *en face* in a short-axis view. A quadricuspid truncal valve is displayed with thickened edges and a central area of noncoaptation. Note the origin of the left main coronary artery from the rightward, posterior sinus (arrow)
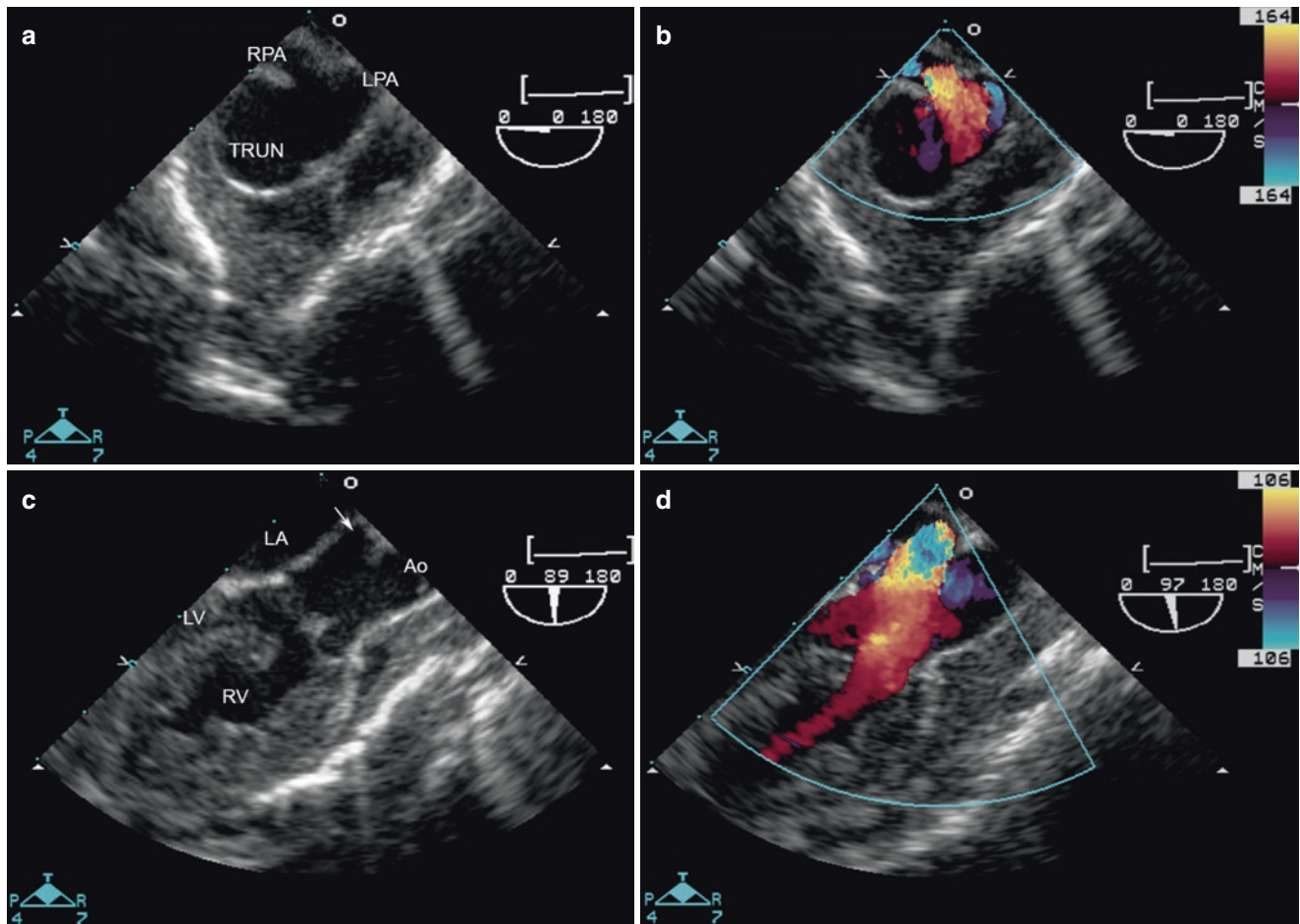
Fig. 14.33 Truncus arteriosus Type "1½" as seen from the ME AoV SAX (*panels* **a** and **b**) and ME AoV LAX (*panels* **c** and **d**) views by 2D and color Doppler imaging. From the short axis views, the origins of the right (*RPA*) and left (*LPA*) pulmonary arteries are seen immediately adjacent to each other, arising from the posterior aspect of the trunk (*TRUN*). From the long-axis views the posterior origin of the pulmonary arteries is also seen (*arrow*), and the truncal root is shown to override the VSD. *Ao* ascending aorta, *LA* left atrium, *LV* left ventricle, *RV* right ventricle

originating from the posterior aspect of the trunk. It can be difficult to display the entire length of the branch PAs by TEE, but significant portions can be visualized using the aforementioned TEE views as well as the UE views (UE PA, UE Ao Arch SAX).

Similar to all conotruncal defects, complementary TEE views (modified ME 4-Ch, ME Bicaval, TG IVC/Hep veins, DTG Atr Sept views) establish the systemic venous connections and confirm the presence of an atrial communication, if present.

It is important to consider that TEE probe placement can be difficult in small infants with TA especially when there is associated 22q11 deletion syndrome [97].

Surgical Considerations

Surgery for TA is usually performed during the neonatal period or early infancy because most patients become symptomatic with congestive symptoms due to pulmonary over-circulation and potentially associated truncal valve problems. Pulmonary vascular obstructive disease can also develop early in patients with this malformation. The specific type of surgical approach is dictated by the anatomy. For the common forms of TA (Types I and II), surgical repair consists of closure of the VSD to the truncal valve, establishing a pathway between the LV and truncal valve—removal of the PAs from the common trunk, closure of the truncal root defect as necessary, and in most cases, placement of a conduit between the RV and the MPA [98–101]. If there is significant truncal valve stenosis or regurgitation, the truncal valve can be addressed during the same operation [102] [103, 104]. In TA Type A4 (of Van Praagh classification scheme), the aortic arch interruption is addressed, in addition to the other aspects of a complete TA repair, detailed above [105–107].

Postoperative TEE helps determine adequacy of the repair. The goals of such imaging are to assure that there is
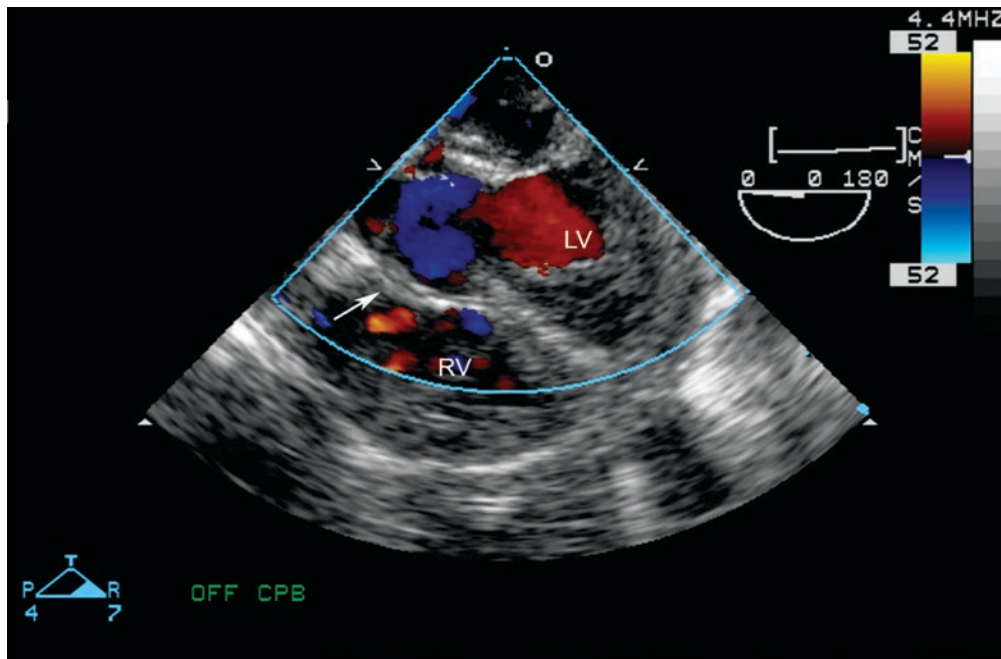
Fig. 14.34 Post truncus arteriosus repair displayed from a ME 5-Ch view. The VSD patch is indicated by the *arrow*; no residual defect was detected by color flow imaging. *LV* left ventricle, *RV* right ventricle
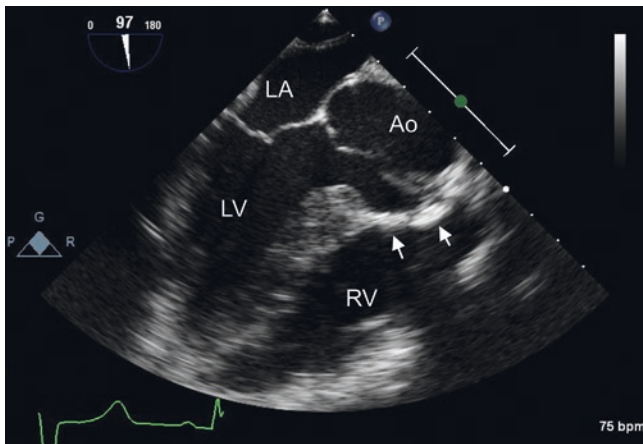

Fig. 14.35 ME LAX view in adult patient with history of truncus arteriosus repair in infancy. Note the dilated truncal root and echogenic VSD patch (*arrows*). *Ao* aorta, *LA* left atrium, *LV* left ventricle, *RV* right ventricle

unobstructed flow from the LV to the truncal root, no significant residual VSD, and unobstructed flow from the RV to the branch PAs. Evaluation of the interatrial septum should be undertaken for residual shunting. It should be noted that in some cases, an intentional small interatrial communication remains, allowing for potential right-to-left shunting and the maintenance of cardiac output during the immediate postoperative period, similar to the case in TOF. In addition, the

post bypass examination is of benefit in the evaluation of truncal valve function (estimation of residual severity of obstruction and/or regurgitation when present preoperatively) in cases where concomitant valve interventions are performed.

The ME 4-Ch and ME 5-Ch views sweeping from an inferior to a superior probe tip position display the location of the VSD patch and color flow Doppler can be used to determine the presence of residual shunting (Figs. 14.34 and 14.35, Videos 14.29 and 14.30). The intramural type VSD previously described can also occur with TA repair [45, 46]. Assessment for a residual VSD should always occur in more than one view. The ME RV In-Out view is quite useful to demonstrate a peri-patch residual leak. In addition, the RV to PA pathway is best seen in this view with a counterclockwise turn of the probe toward the left side of the patient, to almost obtain a ME LAX view (Fig. 14.36, Video 14.31). Doppler interrogation of this pathway can also be performed to assess for outflow tract obstruction in this view as well as the UE PA view. The LV to truncal valve pathway can be seen well in the ME 5-Ch, ME AoV LAX, and ME LAX views (Fig. 14.37, Videos 14.32 and 14.33), along with the assessment of truncal stenosis and regurgitation (Fig. 14.38, Video 14.34) [108]. It is important to evaluate for truncal (neoaortic valve) regurgitation in multiple views as at times one view may not optimally display the severity of the condition. Spectral Doppler
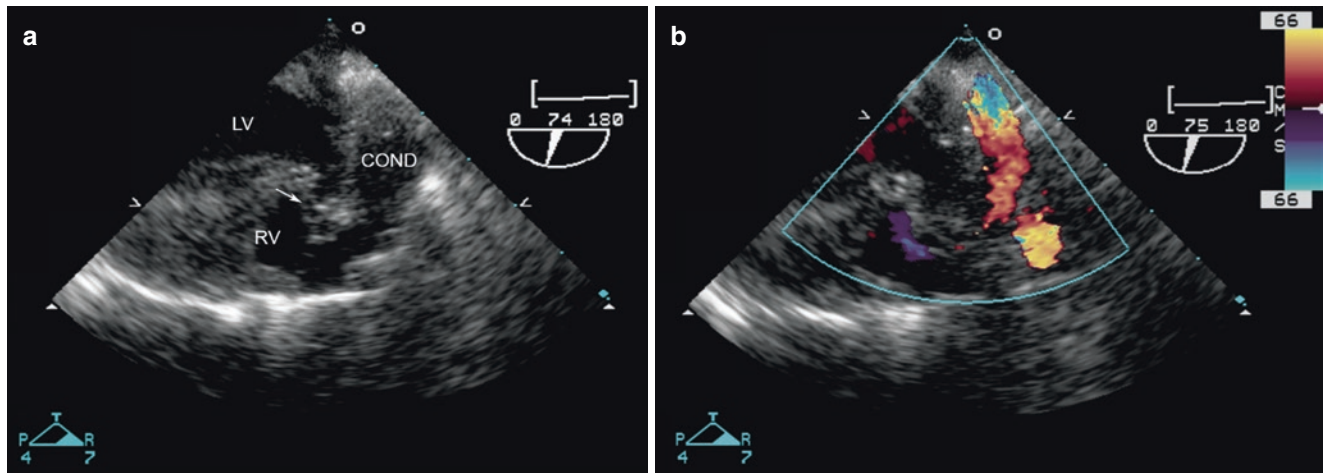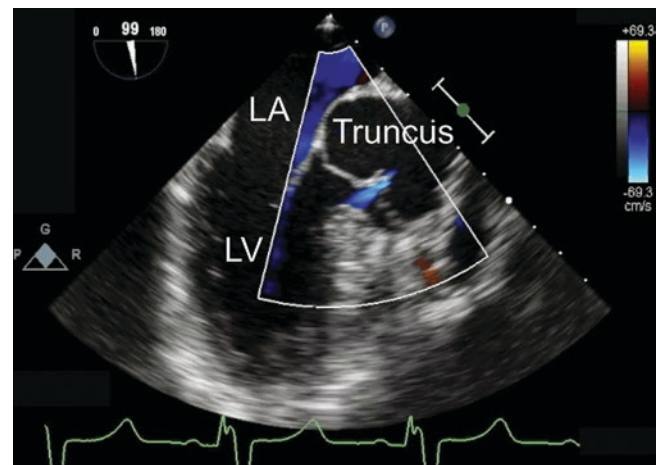
Fig. 14.36 Post truncus arteriosus repair, displayed from a ME LAX view (transducer angle of 74°) by 2D imaging (*panel* **a**) and color flow Doppler (*panel* **b**). The VSD patch (*arrow*) is seen as well as the proximal aspect of the conduit (*COND*) between the right ventricle (*RV*) and the pulmonary artery. *LV* left ventricle
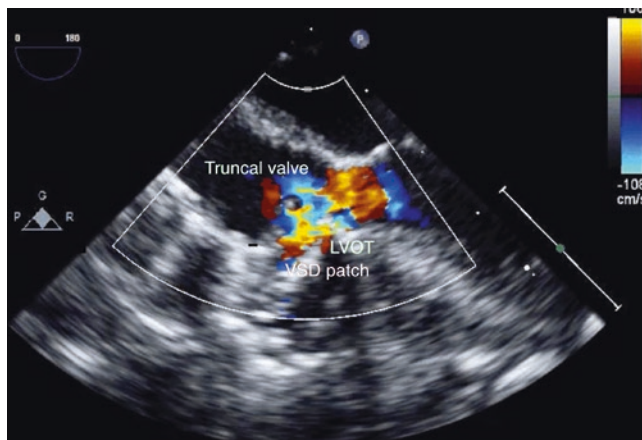
Fig. 14.37 ME 5-Ch view displaying color flow aliasing across the left ventricular outflow tract (*LVOT*) at the region of the ventricular septal defect (*VSD*) patch in a patient post truncus arteriosus repair

Fig. 14.38 ME LAX view displaying trace truncal valve regurgitation in a patient with history of truncus arteriosus repair in infancy. *LA* Left atrium, *LV* left ventricle

interrogation of the aorta, as can be obtained from the descending aorta long-axis view (Desc Ao LAX; transducer angle ~90°–100°), allows for interrogation of retrograde flow during diastole, also serving to assess the severity of truncal valve regurgitation. When available, the DTG RVOT and DTG 5-Ch views can provide visualization of the LVOT and proximal RV to PA conduit, as well as an excellent angle for spectral Doppler assessment. The ME 4-Ch and ME Bicaval views can be used to assess the atrial septum, and the ME 4-Ch, ME 5-Ch, ME RV In-Out, and ME 2-Ch views can facilitate the evaluation of AV valve function. As in all surgical repairs, the assessment of ventricular systolic function is important (as previously noted). Epicardial echocardiography can be useful to assess the branch PAs, as they can become distorted during and after surgery.

Conclusion

The majority of conotruncal defects require surgical intervention. TEE evaluation of these malformations can be performed prior to surgery, during the intraoperative repair (pre and post bypass), and in the follow up assessment of these defects. The flexibility of multiplane imaging allows for unusual angles of interrogation when standard views are not adequate. Importantly, TEE has the potential to help determine the most appropriate surgical pathway for patients with complex anatomy. Outcomes for conotruncal malformations have been improved by our ability to assess repairs in the operating room by TEE and to perform surveillance long after repair particularly when TTE windows are inadequate. Epicardial echocardiography can complement intraoperative TEE in the assessment of these defects and can be particu-

larly useful in the evaluation of the PAs and other vascular structures. As future applications of echocardiography expand, they promise to be particularly applicable to patients with conotruncal anomalies.
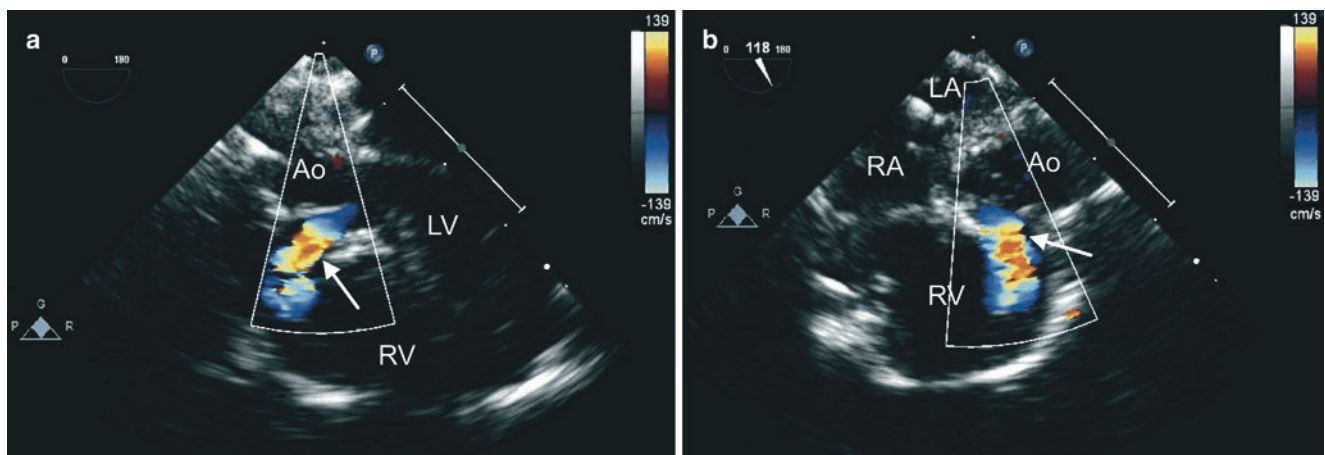
Case-Based Examples

Case #1

Subject: Tetralogy of Fallot with intramural residual VSD

Clinical History: 3-year-old male with history of TOF who presented in the neonatal period with severe RVOT obstruction requiring a prostaglandin infusion. He underwent complete TOF repair with closure of the VSD, relief of RVOT obstruction, and placement of a transannular patch at 4 days of life. Surgical repair was notable for difficult visualization of the VSD. Intraoperative TEE demonstrated an intramural VSD and no residual RVOT obstruction. He developed progressive RVOT obstruction requiring reintervention at 5 months of age at which time closure of the intramural VSD was also undertaken.

TEE Findings:
- ME 5-Ch view with the probe withdrawn to profile the LVOT. The VSD patch is placed in a somewhat horizontal position and a residual intramural VSD is seen by color Doppler interrogation (Fig. 14.39a, Video 14.35).
- ME RV In-Out view at a transducer angle of 118° demonstrating the moderate size residual intramural VSD coursing along the right ventricular trabeculations (Fig. 14.39b, Video 14.36)

Discussion: This case highlights the risk of residual lesions in complex neonatal repairs. Difficult visualization of the VSD upon initial TOF repair during the neonatal period likely resulted in misplacement of the VSD patch, which represents the substrate for an intramural VSD. With time, the amount of shunting across these types of communications can increase [45, 47–49].

Suggested Reading/References
Saedi S, Parsaee M. Intramural ventricular septal defect. Int J Cardiovasc Pract. 2017;2:70-2.

Case #2

Subject: Double-outlet right ventricle with post repair subaortic stenosis

Clinical History: 17-month-old male born with DORV (Taussig Bing type) and coarctation of the aorta. During the neonatal period, he underwent an arterial switch operation with closure of the VSD and aortic arch augmentation. He subsequently developed progressive subaortic stenosis requiring surgical reintervention.

TEE Findings:
- ME LAX view demonstrating a significantly narrowed LVOT associated with VSD patch material (Fig. 14.40, Video 14.37).
- DTG 5-Ch view (image is not in anatomic orientation) demonstrating severe LVOT obstruction with a mean gradient of 41 mmHg. Note the regurgitant spectral Doppler signal (Fig. 14.41).

Fig. 14.39 **Case #1.** *Panel* **a**, ME 5-Ch view to profile the LVOT. The VSD patch is placed in a somewhat horizontal position and a residual intramural VSD is seen by color Doppler interrogation (arrow). *Panel* **b**, ME RV In-Out view at a transducer angle of 118° demonstrating the moderate size residual intramural VSD (*arrow*) coursing along the right ventricular trabeculations. *Ao* aorta, *LA* left atrium, *LV* left ventricle, *RA* right atrium, *RV* right ventricle
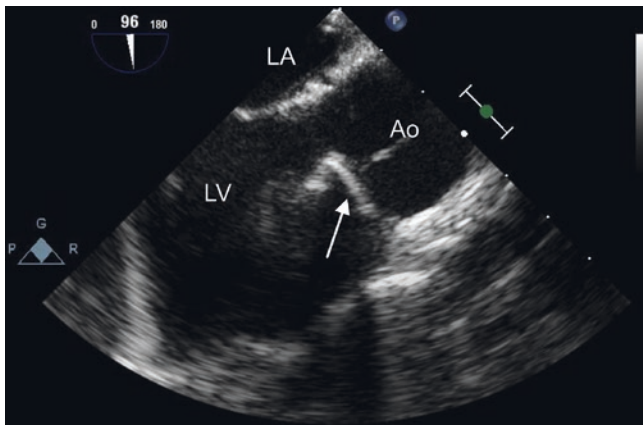
Fig. 14.40 Case #2. ME LAX view demonstrating significantly narrowed LVOT associated with VSD patch material (*arrow*). *Ao* aorta, *LA* left atrium, *LV* left ventricle

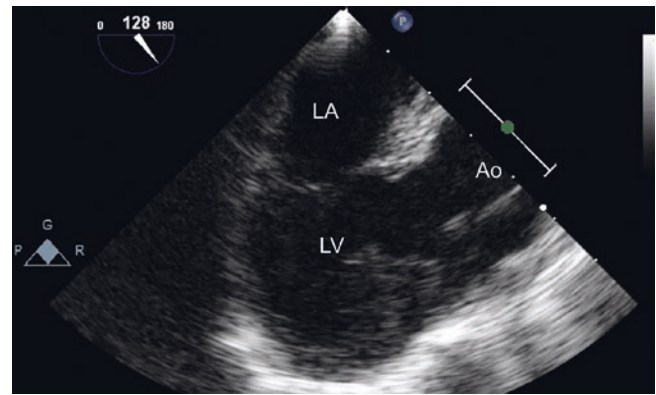**Fig. 14.42** Case #2. After resection of the obstruction there is significant improvement in the appearance of the LVOT in the same patient depicted in Figs. 14.40 and 14.41, with a well-positioned VSD patch as seen in the ME LAX view. *Ao* aorta, *LA* left atrium, *LV* left ventricle

Fig. 14.41 Case #2. DTG 5-Ch view (image is not in anatomic orientation) demonstrating severe LVOT obstruction with a mean gradient of 41 mmHg. Note the regurgitant spectral Doppler signal

- After resection of the obstruction there is significant improvement in the appearance of the LVOT, with a well-positioned VSD patch as seen in the ME LAX view as the probe is rotated towards the left ventricle (Fig. 14.42, Video 14.38) and in the DTG 5-Ch view (Video 14.39). Mild aortic regurgitation is seen.

Discussion: The repair of DORV can be complicated by outflow tract obstruction. The likelihood of problems related to the outflow tracts is influenced by the underlying anatomical substrate and can also be impacted by the surgical intervention. A comprehensive TEE examination is essential in these patients consisting of an evaluation in multiple views and using sweeps that display the pathways between the ventricles and great arteries. Deep transgastric imaging and the use of the spectral Doppler modality are key in this assessment.

Suggested Reading/References

Schwarz F, Blaschczok HC, Sinzobahamvya N et al. The Taussig-Bing anomaly: long-term results. Eur J Cardiothorac Surg. 2013;44:821-7.

Case #3

Subject: Truncus arteriosus with truncal valve regurgitation

Clinical History: 10-year-old male with history of truncus arteriosus repaired at 4 days of life which included truncal valvuloplasty for regurgitation. The RV to PA conduit required replacement at the age of 5 years. He has had preserved left ventricular systolic function but progressive worsening of the truncal valve regurgitation requiring reoperation. A preoperative TEE was performed to evaluate the truncal valve.

TEE Findings:

- The truncal valve is demonstrated in an *en face* orientation in a ME view by 2D and color Doppler as the probe is withdrawn from a ME-5Ch view to the ME AoV SAX position. There is a quadricuspid truncal valve with a central coaptation defect and associated regurgitation (Fig. 14.43a and b, Video 14.40).
- 3D TEE view with color Doppler of the truncal valve demonstrating two coaptation defects, a central one and a second one along the most anterior commissure (Video 14.41).
- The severe nature of the truncal valve regurgitation through a coaptation defect is observed in the ME LAX (Fig. 14.44 and Video 14.42) and DTG 5-Ch (Fig. 14.45 and Video 14.43) views. Note the associated left ventricular dilatation.
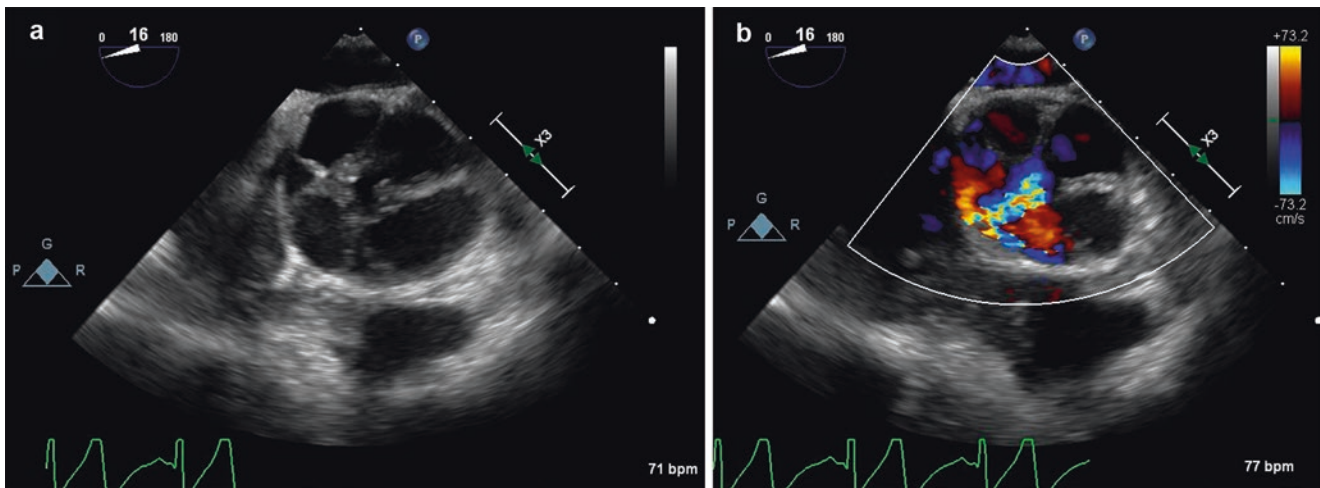
Fig. 14.43 Case #3. *En face view of truncal valve* by 2D (*panel* **a**) and color Doppler (*panel* **b**). A quadricuspid truncal valve is seen with a central coaptation defect and associated regurgitation
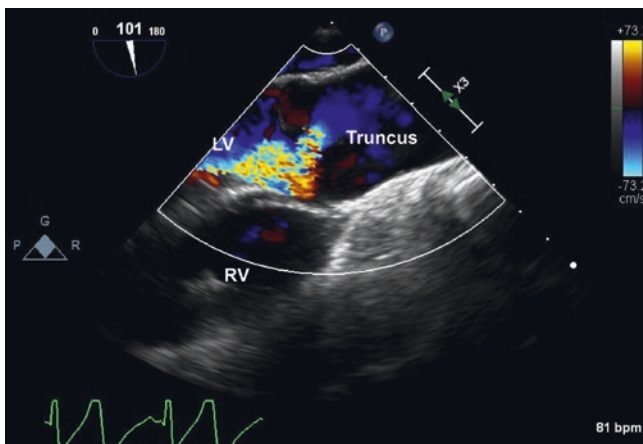
Fig. 14.44 Case #3. ME LAX view in the same patient as shown in Fig. 14.43 displaying severe truncal regurgitation. *LV* left ventricle, *RV* right ventricle

- Spectral Doppler interrogation in the Desc Ao LAX view showing retrograde flow in the descending aorta (Fig. 14.46). The spectral Doppler evaluation complements the color Doppler examination being consistent with significant truncal valve regurgitation.

Discussion: Truncal valve dysfunction, either stenosis or regurgitation, may require concomitant valve interventions at the time of the initial repair in TA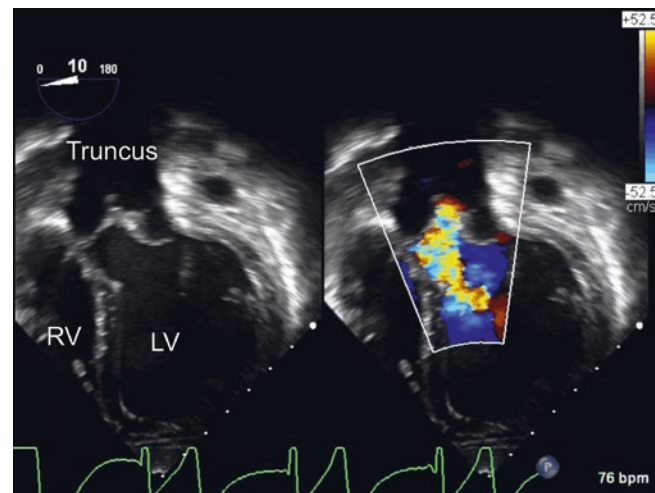 or later on in life. A number of factors have been linked to the need for truncal valve surgery including the presence of a dysplastic valve, an abnormal number of truncal valve cusps, and an anomalous coronary artery pattern. In many cases, a comprehensive anatomical and functional assessment of the truncal valve can be

Fig. 14.45 Case #3. DTG 5-Ch views (2D and color Doppler) in the same patient as shown in Figs. 14.43 and 14.44 depicting severe truncal valve regurgitation. *LV* left ventricle, *RV* right ventricle

performed by TTE. Intraoperative prebypass TEE confirms these findings and it can provide additional details not available by transthoracic imaging. TEE plays an important role in the evaluation of the truncal valve interventions, whether assessing the valve repair for the presence and severity of stenosis or regurgitation or if valve replacement is undertaken.

Suggested Reading/References

Patrick WL, Mainwaring RD, Carrillo SA et al. Anatomic factors associated with truncal valve insufficiency and the need for truncal valve repair. World J Pediatr Congenit Heart Surg. 2016;7:9-15.
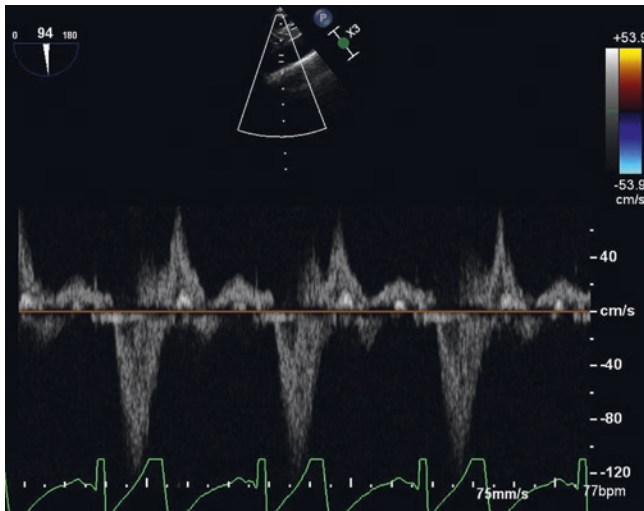
Fig. 14.46 **Case #3.** Spectral Doppler interrogation in the Desc Ao LAX view *s*howing retrograde flow in the descending aorta.

Questions and Answers

1. The characteristics of an intramural VSD include all of the following *EXCEPT*
   a. Patch attached to the RV free wall
   b. Capable of getting larger over time
   c. Associated with increased morbidity and mortality compared to peripatch VSDs
   d. Can occur prior to any surgery
   e. Defects are difficult for the surgeon to visualize

   Answer: d
   Explanation: Intramural defects only occur after surgery, usually for repair of conotruncal defects. They can become larger as the RV trabeculations pull away from the free wall and are difficult for the surgeon to identify through the right atrium or the right ventricle. In some cases, the surgeon must approach these defects through the aorta. Intramural defects are associated with higher morbidity and mortality compared to peripatch VSDs.

2. In DORV with subaortic ventricular septal defect (VSD type), the most common intraoperative complication other than a residual VSD is
   a. Obstruction to the RVOT
   b. Obstruction to the LVOT
   c. Aortic regurgitation
   d. Branch pulmonary artery stenosis
   e. Coronary artery stenosis

   Answer: b
   Explanation: DORV with subaortic VSD typically has conus (muscular tissue) under the aortic valve. Thus, the pathway from the LV to the aorta can become narrowed either because of the subaortic conus or because of the posi-

tion of the VSD patch. Other complications can occur, but this is the one of most concern with this particular anatomy.

3. A foramen ovale may be left open in many forms of conotruncal repairs because
   a. It can augment cardiac output when RV compliance is poor
   b. There is concern for left atrial hypertension
   c. It is too difficult for the surgeon to close
   d. It allows the surgeon to de-air the heart
   e. Potential need for pulmonary vein interventions

   Answer: a
   Explanation: The complete repair of a conotruncal anomaly frequently requires a right ventriculotomy. The RV may be stiff and poorly compliant in this setting. The presence of a small interatrial communication in the form of a foramen ovale allows for right-to-left shunting that augments cardiac output as the RV compliance improves in the postoperative period.

4. The *least* likely finding in the postoperative TEE evaluation following TOF repair is
   a. Residual VSD
   b. RVOT obstruction
   c. Mitral regurgitation
   d. Tricuspid regurgitation
   e. Pulmonary regurgitation

   Answer: c
   Explanation: Definitive repair of TOF consists of VSD closure and repair of the RVOT obstruction. Excluding the presence of residual ventricular level shunting and RVOT obstruction are the primary focus on the postoperative interrogation. The intervention frequently results in pulmonary regurgitation because the patch may be extended across the pulmonary valve annulus. Tricuspid regurgitation can occur as well, because the VSD is frequently repaired through the tricuspid valve or the repair may involve detachment of the valve to access the VSD and later reattachment. In contrast, mitral regurgitation is a very uncommon finding as the surgeon typically does not enter the left side of the heart, although it may occur in the setting of LV dysfunction.

5. All statements regarding truncus arteriosus are true *EXCEPT*
   a. Branch pulmonary artery pattern is variable
   b. Right aortic arch is common
   c. There is more than one classification system
   d. Type II is associated with interrupted aortic arch
   e. The truncal valve is usually abnormal

   Answer: d
   Explanation: Type A4 truncus (Van Praagh classification) is associated with interrupted aortic arch (usually type

B). Truncus arteriosus is associated with a variable branch pulmonary artery pattern, depending upon the type (see Fig. 14.31). A right aortic arch is common, occurring in approximately 25% of patients, and is highly associated with 22q11 deletion. The truncal valve is frequently abnormal, and truncal stenosis and/or regurgitation are frequently associated pathologies.

6. Among TEE views, the one that provides for best assessment of leaflet morphology in a truncal valve is the
   a. ME LAX view
   b. ME Asc Ao SAX view
   c. ME 5-Ch view
   d. ME AoV SAX view
   e. UE Ao Arch SAX

Answer d

Explanation: Leaflet morphology of the truncal valve is variable in truncus arteriosus. Truncal valve interventions may be indicated at the time of complete repair of truncus arteriosus in the presence of severe valve stenosis of regurgitation. The ME AoV SAX view in most cases is ideal for providing detailed information of truncal valve leaflet morphology. The assessment of truncal valve function is complemented by the use of additional views at the midesophageal and deep transgastric levels. A thorough evaluation of the truncal valve should be undertaken using a combination of 2D imaging, color flow, and spectral Doppler modalities.

References

1. Loick HM, Scheld HH, Van Aken H. Impact of perioperative transesophageal echocardiography on cardiac surgery. Thorac Cardiovasc Surg. 1997;45:321–5.
2. Peres M, Pitta ML, Alcaravela J, et al. Transesophageal echocardiography in an emergency setting. A district general hospital experience. Rev Port Cardiol. 2005;24:971–9.
3. Silvestry FE, Kerber RE, Brook MM, et al. Echocardiography-guided interventions. J Am Soc Echocardiogr. 2009;22:213–31. quiz 316
4. Hascoët S, Warin-Fresse K, Baruteau AE, et al. Cardiac imaging of congenital heart diseases during interventional procedures continues to evolve: pros and cons of the main techniques. Arch Cardiovasc Dis. 2016;109:128–42.
5. Van Praagh R. The first Stella Van Praagh memorial lecture: the history and anatomy of tetralogy of Fallot. Semin Thorac Cardiovasc Surg Pediatr Card Surg Annu. 2009:19–38.
6. Anderson RH, Weinberg PM. The clinical anatomy of tetralogy of Fallot. Cardiol Young. 2005;15(Suppl 1):38–47.
7. Michielon G, Marino B, Formigari R, et al. Genetic syndromes and outcome after surgical correction of tetralogy of Fallot. Ann Thorac Surg. 2006;81:968–75.
8. Peyvandi S, Lupo PJ, Garbarini J, et al. 22q11.2 deletions in patients with conotruncal defects: data from 1,610 consecutive cases. Pediatr Cardiol. 2013;34:1687–94.
9. McElhinney DB, Straka M, Goldmuntz E, Zackai EH. Correlation between abnormal cardiac physical examination and echocardiographic findings in neonates with down syndrome. Am J Med Genet. 2002;113:238–41.
10. Braudo JL, Zion MM. Cyanotic spells and loss of consciousness induced by cardiac catheterization in patients with Fallot's tetralogy. Am Heart J. 1960;59:10–8.
11. Hawker RE, Celermajer JM, Cartmill TB. Detection and treatment of inapparent "blue spells" in the seriously ill patient with tetralogy of Fallot. Med J Aust. 1971;2:663–4.
12. Shaddy RE, Viney J, Judd VE, McGough EC. Continuous intravenous phenylephrine infusion for treatment of hypoxemic spells in tetralogy of Fallot. J Pediatr. 1989;114:468–70.
13. Kohli V, Azad S, Sachdev MS, et al. Balloon dilation of the pulmonary valve in premature infants with tetralogy of Fallot. Pediatr Cardiol. 2008;29:946–9.
14. Massoud I, Imam A, Mabrouk A, et al. Palliative balloon valvoplasty of the pulmonary valve in tetralogy of Fallot. Cardiol Young. 1999;9:24–36.
15. Sluysmans T, Neven B, Rubay J, et al. Early balloon dilatation of the pulmonary valve in infants with tetralogy of Fallot. Risks and benefits. Circulation. 1995;91:1506–11.
16. Hirsch JC, Mosca RS, Bove EL. Complete repair of tetralogy of Fallot in the neonate: results in the modern era. Ann Surg. 2000;232:508–14.
17. Kolcz J, Pizarro C. Neonatal repair of tetralogy of Fallot results in improved pulmonary artery development without increased need for reintervention. Eur J Cardiothorac Surg. 2005;28:394–9.
18. Reddy VM, Liddicoat JR, McElhinney DB, Brook MM, Stanger P, Hanley FL. Routine primary repair of tetralogy of Fallot in neonates and infants less than three months of age. Ann Thorac Surg. 1995;60:S592–6.
19. Loomba RS, Buelow MW, Woods RK. Complete repair of tetralogy of Fallot in the neonatal versus non-neonatal period: a meta-analysis. Pediatr Cardiol. 2017;38:893–901.
20. Savla JJ, Faerber JA, Huang YV, et al. 2-year outcomes after complete or staged procedure for tetralogy of Fallot in neonates. J Am Coll Cardiol. 2019;74:1570–9.
21. Schneider M, Zartner P, Sidiropoulos A, Konertz W, Hausdorf G. Stent implantation of the arterial duct in newborns with duct-dependent circulation. Eur Heart J. 1998;19:1401–9.
22. Alwi M, Choo KK, Latiff HA, Kandavello G, Samion H, Mulyadi MD. Initial results and medium-term follow-up of stent implantation of patent ductus arteriosus in duct-dependent pulmonary circulation. J Am Coll Cardiol. 2004;44:438–45.
23. Alwi M. Stenting the ductus arteriosus: case selection, technique and possible complications. Ann Pediatr Cardiol. 2008;1:38–45.
24. Walsh MA, Lee KJ, Chaturvedi R, Van Arsdell GS, Benson LN. Radiofrequency perforation of the right ventricular outflow tract as a palliative strategy for pulmonary atresia with ventricular septal defect. Catheter Cardiovasc Interv. 2007;69:1015–20.
25. Jureidini SB, Appleton RS, Nouri S. Detection of coronary artery abnormalities in tetralogy of Fallot by two-dimensional echocardiography. J Am Coll Cardiol. 1989;14:960–7.
26. Need LR, Powell AJ, del Nido P, Geva T. Coronary echocardiography in tetralogy of Fallot: diagnostic accuracy, resource utilization and surgical implications over 13 years. J Am Coll Cardiol. 2000;36:1371–7.
27. Suzuki A, Ho SY, Anderson RH, Deanfield JE. Further morphologic studies on tetralogy of Fallot, with particular emphasis on the prevalence and structure of the membranous flap. J Thorac Cardiovasc Surg. 1990;99:528–35.
28. Postema PG, Rammeloo LA, van Litsenburg R, Rothuis EG, Hruda J. Left superior vena cava in pediatric cardiology associated with extra-cardiac anomalies. Int J Cardiol. 2008;123:302–6.
29. Vetrano DL, Onder G, Marano R, et al. Unrepaired tetralogy of Fallot in a 73 year old woman. Int J Cardiol. 2013;168:e60–2.

30. Puchalski MD, Lui GK, Miller-Hance WC, et al. Guidelines for performing a comprehensive transesophageal echocardiographic examination in children and all patients with congenital heart disease: recommendations from the American Society of Echocardiography. J Am Soc Echocardiogr. 2019;32:173–215.

31. Knight L, Edwards JE. Right aortic arch. Types and associated cardiac anomalies. Circulation. 1974;50:1047–51.

32. Bacha E. Valve-sparing or valve reconstruction options in tetralogy of Fallot surgery. Semin Thorac Cardiovasc Surg Pediatr Card Surg Annu. 2017;20:79–83.

33. Vida VL, Stellin G. Valve-sparing repair during repair of tetralogy of Fallot: surgical controversies. J Thorac Cardiovasc Surg. 2018;156(2):781.

34. Boni L, García E, Galletti L, et al. Current strategies in tetralogy of Fallot repair: pulmonary valve sparing and evolution of right ventricle/left ventricle pressures ratio. Eur J Cardiothorac Surg. 2009;35:885–9. discussion 889

35. van den Berg J, Hop WC, Strengers JL, et al. Clinical condition at mid-to-late follow-up after transatrial-transpulmonary repair of tetralogy of Fallot. J Thorac Cardiovasc Surg. 2007;133:470–7.

36. Padalino MA, Vida VL, Stellin G. Transatrial-transpulmonary repair of tetralogy of Fallot. Semin Thorac Cardiovasc Surg Pediatr Card Surg Annu. 2009:48–53.

37. Joyce JJ, Hwang EY, Wiles HB, Kline CH, Bradley SM, Crawford FA. Reliability of intraoperative transesophageal echocardiography during tetralogy of Fallot repair. Echocardiography. 2000;17:319–27.

38. Yang SG, Novello R, Nicolson S, et al. Evaluation of ventricular septal defect repair using intraoperative transesophageal echocardiography: frequency and significance of residual defects in infants and children. Echocardiography. 2000;17:681–4.

39. Muhiudeen IA, Roberson DA, Silverman NH, Haas G, Turley K, Cahalan MK. Intraoperative echocardiography in infants and children with congenital cardiac shunt lesions: transesophageal versus epicardial echocardiography. J Am Coll Cardiol. 1990;16:1687–95.

40. Stümper O, Kaulitz R, Sreeram N, et al. Intraoperative transesophageal versus epicardial ultrasound in surgery for congenital heart disease. J Am Soc Echocardiogr. 1990;3:392–401.

41. Dragulescu A, Golding F, Van Arsdell G, et al. The impact of additional epicardial imaging to transesophageal echocardiography on intraoperative detection of residual lesions in congenital heart surgery. J Thorac Cardiovasc Surg. 2012;143:361–7.

42. Manvi VF, Dixit M, Srinivas K, Vagarali A, Patil S, Manvi NG. Accuracy of intraoperative epicardial echocardiography in the assessment of surgical repair of congenital heart defects confirmed. J Cardiovasc Echogr. 2013;23:60–5.

43. Stern KWD, Emani SM, Peek GJ, Geva T, Kutty S. Epicardial echocardiography in pediatric and congenital heart surgery. World J Pediatr Congenit Heart Surg. 2019;10:343–50.

44. Patel JK, Glatz AC, Ghosh RM, et al. Accuracy of transesophageal echocardiography in the identification of postoperative intramural ventricular septal defects. J Thorac Cardiovasc Surg. 2016;152:688–95.

45. Preminger TJ, Sanders SP, van der Velde ME, Castañeda AR, Lock JE. "Intramural" residual interventricular defects after repair of conotruncal malformations. Circulation. 1994;89:236–42.

46. Patel JK, Glatz AC, Ghosh RM, et al. Intramural ventricular septal defect is a distinct clinical entity associated with postoperative morbidity in children after repair of conotruncal anomalies. Circulation. 2015;132:1387–94.

47. Belli E, Houyel L, Serraf A, Lacour-Gayet F, Petit J, Planché C. Transaortic closure of residual intramural ventricular septal defect. Ann Thorac Surg. 2000;69:1496–8.

48. Buratto E, Naimo PS, Konstantinov IE. Intramural ventricular septal defect after repair of conotruncal anomalies: is there light at the end of the tunnel. J Thorac Cardiovasc Surg. 2016;152:696–7.

49. Patel ND, Kim RW, Pornrattanarungsi S, Wong PC. Morphology of intramural ventricular septal defects: clinical imaging and autopsy correlation. Ann Pediatr Cardiol. 2018;11:308–11.

50. Motta P, Miller-Hance WC. Transesophageal echocardiography in tetralogy of Fallot. Semin Cardiothorac Vasc Anesth. 2012;16:70–87.

51. Kaushal SK, Radhakrishanan S, Dagar KS, et al. Significant intraoperative right ventricular outflow gradients after repair for tetralogy of Fallot: to revise or not to revise. Ann Thorac Surg. 1999;68:1705–12. discussion 1712

52. Alhawri KA, Mcmahon CJ, Alrih MM, et al. Atrioventricular septal defect and tetralogy of Fallot - a single tertiary center experience: a retrospective review. Ann Pediatr Cardiol. 2019;12:103–9.

53. Lancellotti P, Tribouilloy C, Hagendorff A, et al. Recommendations for the echocardiographic assessment of native valvular regurgitation: an executive summary from the European Association of Cardiovascular Imaging. Eur Heart J Cardiovasc Imaging. 2013;14:611–44.

54. Zoghbi WA, Adams D, Bonow RO, et al. Recommendations for noninvasive evaluation of native valvular regurgitation: a report from the American Society of Echocardiography developed in collaboration with the Society for Cardiovascular Magnetic Resonance. J Am Soc Echocardiogr. 2017;30:303–71.

55. Fuller S. Tetralogy of Fallot and pulmonary valve replacement: timing and techniques in the asymptomatic patient. Semin Thorac Cardiovasc Surg Pediatr Card Surg Annu. 2014;17:30–7.

56. Suleiman T, Kavinsky CJ, Skerritt C, Kenny D, Ilbawi MN, Caputo M. Recent development in pulmonary valve replacement after tetralogy of Fallot repair: the emergence of hybrid approaches. Front Surg. 2015;2:22.

57. Jones MI, Qureshi SA. Recent advances in transcatheter management of pulmonary regurgitation after surgical repair of tetralogy of Fallot. F1000Res. 2018:7.

58. Walters HL, Mavroudis C, Tchervenkov CI, Jacobs JP, Lacour-Gayet F, Jacobs ML. Congenital heart surgery nomenclature and database project: double outlet right ventricle. Ann Thorac Surg. 2000;69:S249–63.

59. Ebadi A, Spicer DE, Backer CL, Fricker FJ, Anderson RH. Double-outlet right ventricle revisited. J Thorac Cardiovasc Surg. 2017;154:598–604.

60. Bradley TJ, Karamlou T, Kulik A, et al. Determinants of repair type, reintervention, and mortality in 393 children with double-outlet right ventricle. J Thorac Cardiovasc Surg. 2007;134:967–73.

61. Keane JF, Fyler DC. Double outlet right ventricle. In: Keane JF, Fyler DC, Lock J, editors. Nadas' Pediatric cardiology. 2nd ed. Philadelphia: Saunders; 2006. p. 735–41.

62. Ikemoto Y, Nogi S, Teraguchi M, Imamura H, Kobayashi Y. Double-outlet right ventricle with intact ventricular septum. Acta Paediatr Jpn. 1997;39:233–6.

63. Vairo U, Tagliente MR, Fasano ML, Adurno G, Serino W. Double-outlet right ventricle with intact ventricular septum. Ital Heart J. 2001;2:397–400.

64. Geva T, Van Praagh S, Sanders SP, Mayer JE, Van Praagh R. Straddling mitral valve with hypoplastic right ventricle, criss-cross atrioventricular relations, double outlet right ventricle and dextrocardia: morphologic, diagnostic and surgical considerations. J Am Coll Cardiol. 1991;17:1603–12.

65. Wright GE, Maeda K, Silverman NH, Hanley FL, Roth SJ. Double-outlet right ventricle. In: Allen HD, Shaddy RE, Penny DJ, Feltes TF, Cetta F, editors. Moss and Adams' Heart disease in infants, children and adolescents: including the fetus and young adult. 9th ed. Philadelphia: Wolters Kluwer; 2016. p. 1201–15.

66. Pang KJ, Meng H, Hu SS, et al. Echocardiographic classification and surgical approaches to double-outlet right ventricle for great arteries arising almost exclusively from the right ventricle. Tex Heart Inst J. 2017;44:245–51.

67. Oladunjoye O, Piekarski B, Baird C, et al. Repair of double out-let right ventricle: midterm outcomes. J Thorac Cardiovasc Surg. 2019;

68. Anderson RH, Becker AE, Wilcox BR, Macartney FJ, Wilkinson JL. Surgical anatomy of double-outlet right ventricle--a reap-praisal. Am J Cardiol. 1983;52:555–9.

69. Belli E, Serraf A, Lacour-Gayet F, et al. Surgical treatment of subaor-tic stenosis after biventricular repair of double-outlet right ventricle. J Thorac Cardiovasc Surg. 1996;112:1570–8. discussion 1578

70. Khanolkar UB, Kinare SG. Taussig-Bing complex--a pathologic study of eight cases. Indian Heart J. 1990;42:157–60.

71. Serraf A, Lacour-Gayet F, Bruniaux J, et al. Anatomic repair of Taussig-Bing hearts. Circulation. 1991;84:III200–5.

72. Hayes DA, Jones S, Quaegebeur JM, et al. Primary arterial switch operation as a strategy for total correction of Taussig-Bing anom-aly: a 21-year experience. Circulation. 2013;128:S194–8.

73. Uemura H, Yagihara T, Kadohama T, Kawahira Y, Yoshikawa Y. Repair of double outlet right ventricle with doubly-committed ventricular septal defect. Cardiol Young. 2001;11:415–9.

74. Li S, Ma K, Hu S, et al. Surgical outcomes of 380 patients with double outlet right ventricle who underwent biventricular repair. J Thorac Cardiovasc Surg. 2014;148:817–24.

75. Bartram U, Molin DG, Wisse LJ, et al. Double-outlet right ven-tricle and overriding tricuspid valve reflect disturbances of looping, myocardialization, endocardial cushion differentia-tion, and apoptosis in TGF-beta(2)-knockout mice. Circulation. 2001;103:2745–52.

76. Kleinert S, Sano T, Weintraub RG, Mee RB, Karl TR, Wilkinson JL. Anatomic features and surgical strategies in double-outlet right ventricle. Circulation. 1997;96:1233–9.

77. Villemain O, Belli E, Ladouceur M, et al. Impact of anatomic characteristics and initial biventricular surgical strategy on out-comes in various forms of double-outlet right ventricle. J Thorac Cardiovasc Surg. 2016;152:698–706.e3.

78. Castaneda AR, Jonas RA, Mayer JE, Hanley FL. Double-outlet right ventricle. In: Castaneda AR, Jonas RA, Mayer JE, Hanley FL, editors. Cardiac surgery of the neonate and infant. Philadelphia: W.B. Saunders; 1994. p. 445–59.

79. Artrip JH, Sauer H, Campbell DN, et al. Biventricular repair in double outlet right ventricle: surgical results based on the STS-EACTS international nomenclature classification. Eur J Cardiothorac Surg. 2006;29:545–50.

80. Morell VO, Jacobs JP, Quintessenza JA. Aortic translocation in the management of transposition of the great arteries with ventric-ular septal defect and pulmonary stenosis: results and follow-up. Ann Thorac Surg. 2005;79:2089–92. discussion 2092

81. Yeh T, Ramaciotti C, Leonard SR, Roy L, Nikaidoh H. The aortic translocation (Nikaidoh) procedure: midterm results superior to the Rastelli procedure. J Thorac Cardiovasc Surg. 2007;133:461–9.

82. Raju V, Myers PO, Quinonez LG, et al. Aortic root translocation (Nikaidoh procedure): intermediate follow-up and impact of con-duit type. J Thorac Cardiovasc Surg. 2015;149:1349–55.

83. Ventosa-Fernández G, Pérez-Negueruela C, Mayol J, Paradela M, Caffarena-Calvar JM. The Nikaidoh procedure for complex trans-position of the great arteries: short-term follow-up. Cardiol Young. 2017;27:945–50.

84. Kanter KR. The Yasui operation. Oper Tech Thorac Cardiovasc Surg. 2010;15:206–22.

85. Kanter KR, Kirshbom PM, Kogon BE. Biventricular repair with the Yasui operation (Norwood/Rastelli) for systemic outflow tract obstruction with two adequate ventricles. Ann Thorac Surg. 2012;93:1999–2005. discussion 2005

86. Sharma R. Pulmonary artery banding: rationale and possible indi-cations in the current era. Ann Pediatr Cardiol. 2012;5:40–3.

87. Penny DJ, Spicer D, Anderson RH. Common arterial trunk. In: Wernovsky G, Anderson RH, Kumar K, et al., editors. Anderson's

88. Pediatric cardiology. 4th ed. Philadelphia: Churchill Livingstone; 2019. p. 741–54.

89. Van Praagh R, Van Praagh S. The anatomy of common aortico-pulmonary trunk (truncus arteriosus communis) and its embryo-logic implications. A study of 57 necropsy cases. Am J Cardiol. 1965;16:406–25.

89. Cabalka AK, Edwards W, Dearani JA. Truncus Arteriosus. In: Allen HD, Shaddy RE, Penny DJ, Feltes TF, Cetta F, editors. Moss and Adams' Heart disease in infants, children and adolescents: including the fetus and young adult. 9th ed. Philadelphia: Wolters Kluwer; 2016. p. 1053–64.

90. McElhinney DB, Driscoll DA, Emanuel BS, Goldmuntz E. Chromosome 22q11 deletion in patients with truncus arterio-sus. Pediatr Cardiol. 2003;24:569–73.

91. Paris YM, Bhan I, Marx GR, Rhodes J. Truncus arteriosus with a single left ventricle: case report of a previously unrecognized entity. Am Heart J. 1997;133:377–80.

92. Collett RW, Edwards JE. Persistent truncus arteriosus: a clas-sification according to anatomic types. Surg Clin North Am. 1949;29:1245–70.

93. Van Praagh R. Truncus arteriosus: what is it really and how should it be classified. Eur J Cardiothorac Surg. 1987;1:65–70.

94. Jacobs ML. Congenital heart surgery nomenclature and database project: Truncus arteriosus. Ann Thorac Surg. 2000;69:S50–5.

95. Silengo M, Rulli I, Delmonaco AG, Ferrero GB, Pucci A, Sanna R. Truncus arteriosus and isochromosome 8q. Am J Med Genet A. 2005;133A:223–4.

96. Calder L, Van Praagh R, Van Praagh S, et al. Truncus arteriosus communis. Clinical, angiocardiographic, and pathologic findings in 100 patients. Am Heart J. 1976;92:23–38.

97. Wellen SL, Glatz AC, Gaynor JW, Montenegro LM, Cohen MS. Transesophageal echocardiography probe insertion fail-ure in infants undergoing cardiac surgery. Congenit Heart Dis. 2013;8:240–5.

98. Anderson RH. Repair of truncus arteriosus. Eur J Cardiothorac Surg. 2001;20:1080–1.

99. Brown JW, Ruzmetov M, Okada Y, Vijay P, Turrentine MW. Truncus arteriosus repair: outcomes, risk factors, reopera-tion and management. Eur J Cardiothorac Surg. 2001;20:221–7.

100. Mavroudis C, Jonas RA, Bove EL. Personal glimpses into the evo-lution of truncus arteriosus repair. World J Pediatr Congenit Heart Surg. 2015;6:226–38.

101. Asagai S, Inai K, Shinohara T, et al. Long-term outcomes after truncus arteriosus repair: a single-center experience for more than 40 years. Congenit Heart Dis. 2016;11:672–7.

102. Myers PO, Bautista-Hernandez V, del Nido PJ, et al. Surgical repair of truncal valve regurgitation. Eur J Cardiothorac Surg. 2013;44:813–20.

103. Perri G, Filippelli S, Polito A, Di Carlo D, Albanese SB, Carotti A. Repair of incompetent truncal valves: early and mid-term results. Interact Cardiovasc Thorac Surg. 2013;16:808–13.

104. Wei LY, Chen YS, Chiu IS, Huang SC. Repair of a quadricus-pid truncal valve by tricuspidization and reconstruction of right ventricular outflow tract with the excised truncal cusp. J Thorac Cardiovasc Surg. 2018;155:1186–9.

105. Davis JT, Ehrlich R, Blakemore WS, Lev M, Bharati S. Truncus arteriosus with interrupted aortic arch: report of a successful surgi-cal repair. Ann Thorac Surg. 1985;39:82–5.

106. Sano S, Brawn WJ, Mee RB. Repair of truncus arteriosus and interrupted aortic arch. J Card Surg. 1990;5:157–62.

107. Naimo PS, Fricke TA, Yong MS, et al. Outcomes of truncus arte-riosus repair in children: 35 years of experience from a single institution. Semin Thorac Cardiovasc Surg. 2016;28:500–11.

108. Kalavrouziotis G, Purohit M, Ciotti G, Corno AF, Pozzi M. Truncus arteriosus communis: early and midterm results of early primary repair. Ann Thorac Surg. 2006;82:2200–6.